Respective role of plastoglobules and lipid droplets in leaf neutral lipid accumulation during senescence and nitrogen deprivation

Denis Coulon, Houda Nacir, Delphine Bahammou, Juliette Jouhet, Jean-Jacques Bessoule, Laetitia Fouillen, Claire Brehelin

Respective role of plastoglobules and lipid droplets in leaf neutral lipid accumulation during senescence and nitrogen deprivation

Author list:

Denis Coulon[1, §,*], Houda Nacir[1, §], Delphine Bahammou[1], Juliette Jouhet[2], Jean-Jacques Bessoule[1], Laëtitia Fouillen[1], Claire Bréhélin[1,*]

[1] Univ. Bordeaux, CNRS, Laboratoire de Biogenèse Membranaire, UMR 5200, F-33140 Villenave d'Ornon, France.

[2] Univ. Grenoble Alpes, CNRS, CEA, INRAE, IRIG, Laboratoire de Physiologie Cellulaire et Végétale, F-38000 Grenoble, France

[§] These authors share first authorship.

[*]**Correspondence:**

Corresponding authors:

denis.coulon@bordeaux-inp.fr

claire.brehelin@u-bordeaux.fr

ORCIDs:

Claire Bréhélin: 0000-0002-1889-9582

Juliette Jouhet: 0000-0002-4402-2194

Denis Coulon : 0000-0002-3943-1970

Houda Nacir : 0000-0002-1555-2989

Laetitia Fouillen : 0000-0002-1204-9296

Jean-Jacques Bessoule : 0000-0002-5717-5210

Number of figures: **9**

Supporting information: 5 figures, 1 table, 1 method

Tables: 0

Summary:

Upon abiotic stress or senescence, the size and/or abundancy of plastid-localized plastoglobules and cytosolic lipid droplets, both compartments devoted to neutral lipid storage, increase in leaves. Meanwhile, plant lipid metabolism is also perturbed, notably with the degradation of thylakoidal monogalactosyldiacylglycerol (MGDG) and the accumulation of neutral lipids. Although these mechanisms are probably linked, they have never been jointly studied, and the respective roles of plastoglobules and lipid droplets in the plant response to stress are totally unknown. To address this question, we determined and compared the glycerolipid composition of both lipid droplets and plastoglobules, followed their formation in response to nitrogen starvation and studied the kinetics of lipid metabolism in Arabidopsis leaves. Our results demonstrated that plastoglobules preferentially store phytyl-esters, while triacylglycerols (TAGs) and steryl-esters accumulated within lipid droplets. Thanks to a pulse chase labeling approach and lipid analyses of *fatty acid desaturase 2 (fad2)* mutant, we showed that MGDG-derived C18:3 fatty acids were exported to lipid droplets, while MGDG-derived C16:3 fatty acids were stored within plastoglobules. The export of lipids from plastids to lipid droplets was likely facilitated by the physical contact occurring between both organelles, as demonstrated by our electron tomography study. The accumulation of lipid droplets and neutral lipids was transient, suggesting that stress-induced TAGs were remobilized during the plant recovery phase by a mechanism that remains to be explored.

Keywords (5-8): Plastoglobules, lipid droplets, nitrogen starvation, neutral lipids, chloroplast-lipid droplet contact, senescence

Introduction

Leaf senescence contributes a major part to the relocation of nutrients towards storing tissues, such as roots in the case of perennial plants and seeds in the case of annual plants. A major redistribution of lipids in leaves participates in this process, with a reduction in galactolipid content due to the dismantlement of the plastid membranes, a global decrease of up to 80% of total fatty acid (FA) content and an accumulation of TAGs in senescent leaves (Cohen et al., 2022; Kaup et al., 2002; Lin and Oliver, 2008; Yang and Ohlrogge, 2009). In higher plants, TAGs are mainly stored in seeds, pollen and pericarps of oleaginous fruit (*e.g.*, olives or oil palm fruits) and provide a source of energy and carbon necessary for post-germination growth. TAGs also accumulate in leaves under environmental stress, such as heat stress, drought and nitrogen deprivation (Gaude et al., 2007; Higashi et al., 2015; Lee et al., 2019; Mueller et al., 2015; Mueller et al., 2017). TAGs are stored within specialized cytosolic organelles, lipid droplets (LDs), as well as in plastoglobules within plastids. LDs are formed at the ER membrane by the accumulation of TAGs in a lens within the two ER leaflets. When TAG content reaches a threshold, the TAG lens buds from the ER toward the cytosol; this budding is promoted by various factors such as structural proteins or different lipids (recently reviewed in Henne, 2023). The LD structure is identical in all eukaryote cell types, with a core of neutral lipids delimited by a monolayer of polar lipids derived from the cytosolic leaflet of the ER. The monolayer of seed LDs is constituted by different phospholipids (Tzen et al., 1993), while the neutral core is mainly composed of TAGs and steryl-esters (SEs) (Chapman et al., 2019; Horn et al., 2011; Zhou et al., 2019) but may also contain specific lipids, for example wax esters in jojoba seeds (Miwa, 1971). LDs are also present in other plant organs, such as leaves and roots, but in much lower abundance. LD abundancy in leaves varies during the diurnal cycle (Gidda et al., 2016), with an accumulation of LDs at the end of the dark period, suggesting the origin of these LDs from the recycling of membranes that occurs during the night rather than from *de novo* FA synthesis that takes place during the photosynthetic phase. LDs accumulate in leaves in response to various stress conditions, such as heat and cold stress (Gidda et al., 2016), nitrogen starvation (Brocard et al., 2017; Coulon et al., 2020), and fungus infection (Shimada et al., 2014), but also during natural senescence (Brocard et al., 2017; Shimada et al., 2015; Zhang et al., 2020). Although numerous studies on leaf LDs have been carried out, the exact lipid composition of these LDs, which probably differs from seed LDs, is still unknown.

Plastoglobules have a structure similar to LDs, with the stromal leaflet of the thylakoid membrane surrounding the neutral lipid core (Austin et al., 2006). Similar to LDs, they increase in abundance and/or size in response, for example, to high light, drought and nitrogen deprivation, but also during senescence (reviewed in Bréhélin and Kessler, 2008; van Wijk and Kessler, 2017). The lipid composition of plastoglobules is not clearly established and seems to vary according to the type of

plastid or growth conditions. With regard to the polar lipid monolayer, the identity and relative content of phospholipids are unclear (Deruère et al., 1994; Hansmann and Sitte, 1982; Lichtenthaler, 1968; Tevini and Steinmüller, 1985; Wu et al., 1997). Several studies have described the presence of galactolipids in plastoglobules (Greenwood et al., 1963; Hansmann and Sitte, 1982; Hernández-Pinzón et al., 1999; Leggett Bailey and Whyborn, 1963; Lichtenthaler, 1968). However, some authors have suggested that galactolipids can result from contamination by thylakoid membranes (Tevini and Steinmüller, 1985; Tevini and Steinmüller, 1985), and their actual presence in the plastoglobules remains to be firmly confirmed. TAGs are reported to be abundant constituents of plastoglobules in various plastids, such as spinach chloroplasts (Steinmüller and Tevini, 1985), *Viola* and *Sarotamnus* chromoplasts (Hansmann and Sitte, 1982; Steinmüller and Tevini, 1985), and wheat etioplasts (Dahlin and Ryberg, 1986), with a sharp decrease of TAG content during senescence in the plastoglobules of *Fagus sylvatica* leaves (Tevini and Steinmüller, 1985). It is now well established that the neutral lipid core of plastoglobules also contains prenyl quinones, such as plastoquinone, tocopherols (Greenwood et al., 1963; Leggett Bailey and Whyborn, 1963; Lichtenthaler, 1968; Steinmüller and Tevini, 1985; Vidi et al., 2006; Zbierzak et al., 2009), and phylloquinone (Lohmann et al., 2006), as well as fatty acid phytyl-esters (Gaude et al., 2007; Lippold et al., 2012). Chromoplast plastoglobules also store various carotenoids and carotenoid esters (Morelli et al., 2023; reviewed in van Wijk and Kessler, 2017; Zita et al., 2022), which are responsible for fruit color.

The decrease in FA synthesis and galactolipid content, concomitant with an increase in TAG and phytyl-ester content in leaves, in addition to the presence of larger and/or more abundant plastoglobules and the appearance of newly formed LDs, during senescence or under stress conditions, suggest a role for both plastoglobules and LDs as a buffer reservoir for FAs resulting from membrane degradation (Ischebeck et al., 2020; Rottet et al., 2015; reviewed in Yu et al., 2021). However, the respective roles of LDs and plastoglobules in the storage of neutral lipids have never been explored in parallel. TAGs are assembled at the ER through two main pathways. In the Kennedy pathway, two acyltransferases, the GLYCEROL-3-PHOSPHATE ACYLTRANSFERASE (GPAT) and the LYSO-PHOSPHATIDIC ACID ACYLTRANSFERASE (LPAT), sequentially esterify two acyl-CoAs to the glycerol 3-phosphate to produce phosphatidic acid (PA), which is then dephosphorylated by the PHOSPHATIDIC ACID PHOSPHATASE (PAP) to give diacylglycerol (DAG). The DIACYLGLYCEROL ACYLTRANSFERASE (DGAT) subsequently catalyzes the acylation of DAG to TAG. The second pathway does not use acyl-CoA as acyl donor but involves the PHOSPHOLIPID:DIACYLGLYCEROL ACYLTRANSFERASE (PDAT) which catalyzed the transfer of an acyl group from the phosphatidylcholine to DAG (reviewed in Xu and Shanklin, 2016). In addition, some TAG synthesis is also believed to occur in the plastid (Kaup et al., 2002; Lippold et al., 2012). The synthesis of SEs is

115 catalyzed either by an ACYL-COA:STEROL ACYLTRANSFERASE (ASAT) or a PHOSPHOLIPID:STEROL
116 ACYLTRANSFERASE (PSAT) depending on the acyl donor substrate (Reviewed in Ferrer et al., 2017). In
117 Arabidopsis, phytyl-ester synthesis is catalyzed by PHYTYL-ESTER SYNTHASES PES1 and PES2 (Lippold
118 et al., 2012) that are located at the plastoglobules (Vidi et al., 2006; Ytterberg et al., 2006).TAG,
119 steryl-, and phytyl-ester biosynthesis are thought to play a protective role against cytotoxic lipid
120 intermediates (*e.g.,* free FAs (FFAs) and phytol) formed during membrane degradation or lipid
121 remodeling (Bouvier-Navé et al., 2010; Fan et al., 2017; Lu et al., 2020). In addition, neutral lipids
122 accumulated in response to stress conditions probably play important roles during the post-stress
123 recovery phase by providing FAs to facilitate membrane reconstruction or for energy supply through
124 the β-oxidation pathway (Yu et al., 2021; reviewed in Zienkiewicz and Zienkiewicz, 2020).

125 To gain insight into the respective importance of plastoglobules and LDs under conditions that induce
126 thylakoid dismantlement and neutral lipid storage, we monitored the lipid composition of
127 Arabidopsis leaves during natural senescence, senescence artificially induced by nitrogen starvation
128 and reversion after nitrogen supplementation. We compared the lipid composition of both
129 compartments and established that TAGs were mostly stored in LDs, while plastoglobules were
130 dedicated to the storage of phytyl-esters. We showed that during senescence, FAs derived from the
131 degradation of MGDG segregated between the plastoglobules and the LDs, with C16:3 FAs remaining
132 in the plastids, while C18:3 FAs were exported to LDs, probably through the contact sites between
133 plastids and LDs, as shown by electron tomography.

134

Materiel and methods

Plant material and culture conditions:

Arabidopsis thaliana ecotype Columbia (Col-0) were grown as described in (Brocard et al., 2017) at high density on soil in long day conditions (16h light /8h dark), 100 µmol of photon.m^{-2}.s^{-1} at 20-22°C and 65% humidity.

For nitrogen starvation assays, sterile *A. thaliana* seeds were sown on half strength Murashige and Skoog (MS½) medium and grown in long day conditions, at 20–22°C, 16h/8h light/dark cycle for two weeks. Then plantlets were transferred on synthetic minimal medium deprived of nitrogen [0.8% agarose, 1% sucrose, 1mM $MgSO_4$, 1mM KH_2PO_4, 25µM Fe-EDTA, 35µM H_3BO_3, 7µM $MnCl_2$, 0.25µM $CuSO_4$, 0.5µM $ZnSO_4$, 0.1µM Na_2MoO_4, 5µM NaCl, 5nM $CoCl_2$, 1mM $CaCl_2$ and 2.5mM KCl] (Gaude et al., 2007), grown for 10 days more, and transferred back to MS½ plates to recover for 10 days. Note that control plantlets were grown simultaneously and similarly transplanted but in new MS½ plates.

Lipid analyses

For analysis of plant extracts, total lipids from aerial parts were extracted by Folch method (Folch et al., 1957) after phospholipase D inactivation using hot isopropanol, as described in Coulon et al. (2020). For LD and plastoglobule lipid analyses, neutral and polar lipids from the total lipid extract were separated by liquid/liquid extraction as described in Coulon and Bréhélin (2021). The different lipid classes are then separated by thin layer chromatography (TLC). For neutral lipid analyses of nitrogen starved plantlets, plates were developed in hexane:diethyl ether:acetic acid (45:7.5:1, v/v/v) according to Juguelin et al. (1986). For neutral lipid analyses of LDs or plastoglobules, and of senescent leaves, plates were developed firstly in Toluene to a height of 10 cm, then in hexane:diethyl ether:acetic acid (45:7.5:1, v/v/v) to a height of 5 cm (Coulon et al., 2020) to allow the separation of phytyl-esters from steryl-esters. Polar lipids were separated with a Vitiello-Zanetta solvent mixture (Vitiello and Zanetta, 1978). The lipids were visualized with primuline under UV light. After FA trans-esterification, lipids were quantified by gas chromatography (Agilent 7890 gas chromatograph equipped with a Carbowax column Alltech Associates, Deerfield, IL, USA) coupled to a flame ionization detector (FID) as described in (Coulon et al., 2020). The retention times of FA-methyl esters were determined by comparison with standards, and were quantified using heptadecanoic acid methyl ester as standard.

Estimation of the lipid droplet composition:

Analysis of the purified LD fraction revealed the presence of phytyl-esters (from 17,9 to 37,6 %mol, depending to the LD preparation), which we assumed to be solely the result of contamination by plastoglobules. Consequently, the LD fraction is also contaminated by the MAGs, DAGs, FFAs, TAGs and SEs contained in plastoglobules. In plastoglobules, phytyl-esters represent 75.2% on average of the neutral lipids. Knowing the relative composition of the different other neutral lipids in plastoglobules, and the amount of phytyl-esters detected in LDs, we then calculated the content (in moles) of each contaminating lipids in each LD fraction (n=5), with the formula:

$$contaminating\ lipid\ in\ LD\ fraction\#N(mol) = \frac{average\ \%\ of\ the\ considered\ lipid\ in\ plastoglobules \times FAPEs\ in\ LD\ fraction\#N\ (mol)}{average\ \%\ of\ FAPEs\ in\ plastoglobules}$$

The neutral lipid content of the LDs was then calculated by subtracting the content of each contaminating neutral lipid in LDs to the initial values. Finally, the molar distribution of LD neutral lipids, the mean and the standard deviation were calculated.

Liquid chromatography – Mass spectrometry (LC-MS/MS) analyses

For the analysis of galactolipids and steryl-esters by LC-MS/MS, internal standards (17:0 cholesteryl ester and 17:0/14:1 phosphatidylcholine (PC) from Avanti Polar Lipids) were added to lipid extract and LC-MS/MS (multiple reaction monitoring mode) analyses were performed with a QTRAP 6500 (ABSciex) mass spectrometer coupled to a LC system (1290 Infinity II, Agilent) in positive ion mode. The areas of LC peaks were determined using MultiQuant software (version 2.1; ABSciex) for relative lipid quantification.

For the analysis of phospholipids by LC-MS/MS, internal standard (18:0-18:0 phosphatidylethanolamine (PE) and 16:0-18:0 sulfoquinovosyldiacylglycerol (SQDG) extracted from spinach thylakoid (Demé et al., 2014) and hydrogenated as described in Buseman et al (2006)) were added to lipid extract. LC-MS/MS (multiple reaction monitoring mode) analyses were performed in positive ion mode with a 6460 triple quadrupole mass spectrometer (Agilent) equipped with a Jet stream electrospray ion source and coupled to an Agilent 1200 HPLC system. Mass spectra were processed by MassHunter Workstation software (Agilent) for identification and quantification of lipids. Lipid amounts (pmol) were corrected for response differences between internal standards and endogenous lipids and by comparison with a quality control (QC). QC extract correspond to a known lipid extract from Arabidopsis cell culture qualified and quantified by TLC and GC-FID as described by Jouhet et al. (2017). For a complete description of the LC-MS/MS methods used in this paper, see Methods S1.

Transmission electron microscopy (TEM) imagery and Tomography

Chemical fixation of leaves was performed as described in Brocard et al. (2017). Briefly, leaves were fixed in 2.5% Glutaraldehyde, post-fixed by 1% OsO_4 and embedded in SPURR (Electron Microscopy Science, EMS) resin. Ultrathin sections of 80 nm thickness were obtained with ultramicrotome LEICA EM UC7. Transmission electron microscope FEI Tecnai G2 Spirit TWIN 120kV equipped with a CCD 16Mpixels Eagle 4k camera was used for acquisition (120kV). Image analysis was performed with ImageJ software (Schneider et al., 2012). For electron tomography, FEI software was used for tilt series acquisition, Alignment and backprojection steps were respectively achieved with IMOD and tomoJ softwares, and OSART algorithm with 100 iterations was used.

LD and plastoglobules purification

LD and plastoglobules were purified from 6-week-old Arabidopsis leaves by floatation on sucrose gradients, as described in Brocard et al. (2017) and Coulon and Bréhélin (2021) respectively. Briefly, for LD purification leaves were homogenized in cold G-20 buffer (100 mM Tricine (pH7.5), 10 mM KCl, 1 mM EDTA, 1 mM PMSF, plant protease inhibitor cocktail (Sigma), and 20% sucrose), filtered through two layers of cheese cloth and one layer of Miracloth (Calbiochem) and centrifuged at 100 000 g for 30 min. The floating lipid pad was collected and resuspended in 10 mL G-20 buffer using a Potter homogenizer, covered with G-15 buffer (G-buffer with 15% sucrose) and G-5 buffer (G buffer with 5 % sucrose), and centrifuged 50 min at 150 000 g. This step was repeated once. Finally, the floating lipid pad was resuspended in 5 mL G-20 buffer with a Potter homogenizer, covered with G-0 buffer (G buffer without sucrose), and centrifuged 50 min at 150 000 g. The final floating lipid pad constituted the enriched LD fraction, and was stored at -80°C until further analyses. For plastoglobule purification, leaves were homogenized in HB buffer (450 mM sorbitol, 20 mM Tricine-KOH pH 8.4, 10 mM EDTA, 10 mM $NaHCO_3$, 1 mM $MnCl_2$, 5 mM Na-ascorbate, 0.05% (w/v) bovine serum albumin, 1 mM PMSF, plant protease inhibitor cocktail), filtered as for LD purification and centrifuged for 8 min at 1,000 g. Pelleted chloroplasts were resuspended in TrE buffer (5 mM Tricine-KOH pH 7.5, 0.2 mM EDTA, 0.2 mM DTT) and centrifuged for 10 min at 2,700 g. The chloroplast pellet was resuspended in 0.2 M sucrose/TrE, homogenized in a 50 mL Potter and centrifuged for 1h at 100,000g. The pellet of plastid membranes was resuspended in 45% sucrose/TrE buffer, poored on a gradient of 38 %, 20%, 15% and 5% sucrose, and centrifuged overnight at 100,000 g. The floating plastoglobules are homogenized in 45% sucrose/TrE buffer and finally washed on a gradient of 15%, 5% and 0% sucrose.

Protein analyses

For immunoblot experiments, proteins extracted according to Rensink et al. (1998) and concentrated by chloroforme-methanol precipitation (Wessel and Flugge, 1984), were separated by SDS-PAGE and blotted onto nitrocellulose membrane. Blots were probed with sera raised against plastoglobule, ER, plastid envelope or thylakoid markers, respectively AtFBN1b (Vidi et al., 2006), BiP (Höfte and Chrispeels, 1992), AtToc75 (Hiltbrunner et al., 2001), or P16 (Vallon et al., 1986). Proteins were quantified either according to the Bradford method (Bradford, 1976) or the QuantiPro BCA assay kit manual (Sigma).

Preparation of anti-AtLDAP1 serum

ORFs clones of *AtLDAP1* (U17438) in *pENTR* vector were obtained from ABRC center and verified by sequencing. AtLDAP1 ORF was then transferred by GATEWAY® recombinational cloning technology in frame with the included 6xHistidine tag of the pHGWA vector (Busso et al., 2005). The full-length protein was expressed in Escherichia coli BL21 (DE3) (Novagen) and purified under denaturing conditions by nickel nitrilotriacetic acid affinity chromatography (Qiagen, Basel, Switzerland) according to the manufacturer's recommendations. Polyclonal antibodies were produced in rabbit (Covalab, Villeurbanne, France).

Radiolabeling

Two-week-old plantlets grown on MS½ medium were pulse-labeled by incubation with 7 mL MS½ medium supplemented with [^{14}C] acetate (20 µCi) for 2h. Then, plantlets were rinsed three times in 7 mL MS½ medium to remove the excess of [^{14}C] acetate. The chase was done by transferring plantlets either on synthetic minimal medium depleted of nitrogen or on MS½ medium for 10 days. After lipid extraction and separation by TLC, the radioactivity incorporated into neutral and polar lipids was quantified using a Typhoon FLA9500 (GE Heathcare).

Results:

During Arabidopsis leaf ageing neutral lipid content increases and both plastoglobules and LDs accumulate

To monitor the lipid composition of *Arabidopsis* leaves in parallel with the accumulation of plastoglobules and LDs, we grew *Arabidopsis* plantlets for 6 weeks on soil at high density. At the end of these 6 weeks, the plantlets entered senescence but also underwent stress conditions, probably due to the high density, as shown by the purple color of some leaves (Fig. 1A). Ultrastructural study of these 6-week-old plantlets showed that the leaves were at different stages of senescence, with more or less pronounced dismantling of the thylakoid membranes (Fig. 1B). An average of only 0.02 LD per cross section of parenchyma cells was observed in parenchyma cells of 3-week-old leaves whereas 6-week-old green leaves had an average of 1.27 LD per cross section of parenchyma cell and an LD mean diameter of 817 (±251) nm (Fig. 1C). In parallel, the size of plastoglobules increased considerably from a mean diameter of 70 (±14) nm in 3-week-old leaves to 226 (±59) nm in the most senescent 6-week-old leaves. The polar and neutral lipid composition showed a decrease in MGDG and phosphatidylglycerol (PG)/PE content in the 6-week-old plantlets compared to the 4-week-old plantlets, in parallel with an accumulation of neutral lipids, mainly TAGs, steryl- and phytyl-esters with a 28-, 6- and 18-fold increase, respectively (Fig. 1D). Unlike MGDG, the digalactosyldiacylglycerol (DGDG) content was not significantly affected. The compositions of MGDG and DGDG were stable during leaf aging (Figs. 2 and S1), while a decrease in relative C16:0 content was observed in TAGs and phytyl-esters, in favor of an increase in relative C16:3 content (from 61% to 72%) for phytyl-esters and C18:3 (from 43% to 61%) for TAGs. A slight increase in relative C18:3 content (from 32% to 36%) in SEs was also observed, concomitant with a decrease in C18:2 content (from 38% to 26%). These data suggest that TAGs, steryl- and phytyl-esters, which accumulated in senescing leaves, are formed mainly by esterification of MGDG-derived C16:3 and C18:3 FAs, as previously suggested during freezing or heat stress (Moellering et al., 2010; Mueller et al., 2017).

Plastoglobules from 6-week-old leaves accumulate mostly phytyl-esters and contain a limited amount of TAGs and SEs

To determine which neutral lipids accumulate during senescence in plastoglobules and LDs, we purified both compartments from 6-week-old Arabidopsis leaves and determined their glycerolipid composition. The fraction purity was assessed by immunoblot (Fig. 3A) with Golgi, ER, plastid membranes and plastoglobule markers. To obtain an LD marker, we raised serum against Arabidopsis LIPID DROPLET ASSOCIATED PROTEIN1 (AtLDAP1), a protein specific to leaf LDs (Brocard et al., 2017; Gidda et al., 2016). As shown in Fig. 3A, the plastoglobule fraction was free of any membrane or LD

contaminant. We then determined the neutral lipid composition of the plastoglobules by TLC/GC-FID (Fig. 3B). Surprisingly, the neutral lipids in plastoglobules of 6-week-old leaves contained less than 2 mol% of TAGs but were mainly composed of phytyl-esters (75 mol%), with SEs (7 mol%), some FFAs (7 mol%), MAG (7 mol%) and DAG (2 mol%). The TAGs of the plastoglobules (Fig. 4A) had a different composition to that of the total leaves (Fig. 2B), with only 10% and 18% C18:2 and C18:3, respectively, in the plastoglobules compared with 21% and 43% in the leaves, but an enrichment in C16:0, C16:2, C16:3, C18:0 and C18:1. The presence of phytyl-esters in plastoglobules was expected, as previously reported by Gaude et al. (2007). Their FA composition (Fig. 4B) was similar to that of Gaude's study, with a large majority of C16:3. The presence of SEs in plastoglobules was more surprising, as SEs are mainly found in mitochondrial and nuclear membranes, microsomes, and cytosolic LDs (Ferrer et al., 2017). However, their FA composition was different between plastoglobules and LDs, with enrichment of C14:0 and C16:3 in plastoglobules and C18:3 in LDs. To confirm the identity of SEs in plastoglobules, we performed a detailed lipidomic profiling of SEs using LC-MS on lipid extracts from plastoglobules. The LC-MS data confirmed the genuine presence of specific SEs in plastoglobules, such as C14:0-sitosterol and C16:2-sitosterol, and an enrichment of C16:3 SEs at the expense of C18:3 SEs (Fig. 4D). It should be noted that the SE acyl distribution determined by LC-MS differed from that obtained by GC-FID. In particular, saturated C16:0- and C18:0-SEs were not found by LC-MS analysis while detected in significant amounts by GC-FID. LC-MS quantification depends on the ionization yield of the studied molecule, which varies depending on the nature of the molecule (Jouhet et al., 2017). We compared the detection of C18:0-, C18:1-, and C18:2-cholesterol ester standards by LC-MS and observed that the ionization yield of saturated C18:0-cholesterol ester is 10 times lower than that of C18:2-cholesterol ester (Fig. S2), while the amount of each standard was similar according to the quantification performed by GC-FID. Such underestimation by LC-MS of saturated cholesterol esters certainly also applies for other SEs and explains the difference of SE composition observed between LC-MS and GC-FID.

MGDGs, DGDGs and PGs were detected in plastoglobules, but their quantity was below the threshold to be quantified by GC-FID. Therefore, we determined by LC-MS the distribution of the molecular species in each polar lipid class. While the proportion of each molecular species constituting DGDG in the plastoglobules (Fig. 5A) was similar to that in the thylakoids, the proportion of molecular species of MGDG was significantly different (Fig. 5B), with a particular enrichment of MGDG 36:6 in the plastoglobules (49% in the plastoglobules and 38% in the thylakoids). Furthermore, according to our LC-MS measurements, the plastoglobule MGDG/DGDG ratio equaled 3:1, whereas it was around 1:1 in the thylakoids (Fig. 5C). These results suggest that galactolipids are not contaminants but genuine components of the plastoglobule monolayer. The MGDG/DGDG ratio of 1 obtained for thylakoids by LC-MS in this study does not correspond to an absolute quantification of MGDG and DGDG, and is

given as an indication for comparison between the different analyzed fractions. Indeed, as explained above, the ionization yield differs depending on the nature of the molecule analyzed and an absolute quantification by LC-MS is not possible. This explains the difference with the value of the MGDG/DGDG ratio, which is generally estimated between 2 and 3 for Arabidopsis leaves (Dormann et al., 1995; Jarvis et al., 2000; Yu et al., 2020). The composition of the phospholipids present in the plastoglobules was also determined by LC-MS, and a slight enrichment in saturated FAs in the plastoglobule PG was observed compared with those of the thylakoids (Fig. S3).

LDs are mostly comprised of TAGs and steryl-esters

The immunoblots we performed on the LD-enriched fraction (Fig. 3A) showed that it also contained plastoglobules, as noted in our previous proteomic study (Brocard et al., 2017). This contamination originates from the inevitable chloroplast breakage that occurs during LD purification, releasing some plastoglobules. Nevertheless, we established the glycerolipid composition of this LD-enriched fraction (Fig. 3C and D) in a similar way to that achieved with the plastoglobules and were able to determine the proportion of plastoglobule contamination in the LD lipidome (see below).

In contrast to plastoglobules, the neutral lipids in the LD-enriched fraction consisted mainly of SEs and TAGs (Fig. 3C), but phytyl-esters accounted for 29%mol of the total lipid content. Phytyl-esters are wax esters containing phytol and are located in the plastids, particularly in the plastoglobules (Gaude et al., 2007). Thus, we hypothesized that phytyl-esters in the LD-enriched fraction originated from contamination by plastoglobules. This was confirmed by the FA composition of the phytyl-esters, which was similar to that of the plastoglobule phytyl-esters (Fig. 4B). With this premise and our analysis of the plastoglobules showing that phytyl-esters represented 75%mol of the total lipid content of the plastoglobules, we recalculated the neutral lipid composition of the LD-enriched fraction by excluding phytyl-esters and the proportion of other individual neutral lipids originating from contamination by the plastoglobules. The proportion of TAGs and SEs in the LDs was then estimated at 26 and 65%mol, respectively (Fig. 3D). The FA composition of TAGs in LDs (Fig. 4B) was similar to the composition of TAGs in 6-week-old leaves (Fig. 2B) and was totally different from TAGs in plastoglobules, with, for example, a large majority of C18:3 (58%) and C18:2 (18%) in LDs compared with 18 and 10%, respectively, in plastoglobules. These results imply that most of the leaf TAGs are stored in LDs and that the small amount of TAGs found in the plastoglobules, with their specific FA composition, probably originates from a different biosynthetic pathway.

Few quantities of MGDG and DGDG were detected in the LD-enriched fraction. The distributions of their molecular species were determined by LC-MS and found to be significantly different from those of plastoglobules and thylakoids (Fig. 5), with enrichment in MGDG 34:6 (57, 32 and 44% in LDs, plastoglobules and thylakoids, respectively) and DGDG 34:3 (37, 23 and 20% in LDs, plastoglobules

and thylakoids, respectively) and depletion in MGDG 36:6 (23, 49 and 38% in LDs, plastoglobules and thylakoids, respectively) and DGDG 36:6 (24, 53 and 51% in LDs, plastoglobules and thylakoids, respectively). The presence of galactolipids in extra-plastidial LDs was surprising, but their specific FA compositions suggest that they were not derived from contamination by plastoglobules or thylakoids but rather were true constituents of LDs. This suggests an export of lipids across the plastidial envelope to the LDs and possibly other extraplastidial compartments, as previously described during phosphate starvation (Härtel et al., 2000; Klaus et al., 2002).

More generally, the overall FA compositions of neutral lipids differed in plastoglobules and LDs (Fig. 4E), with the majority of C16:3 (56%) in plastoglobules, whereas neutral lipids in LDs were mainly composed of C18:3 (49%) and C18:2 (20%), suggesting that the neutral lipids contained in these two compartments did not have the same origin.

MGDG-derived FAs are incorporated into TAG and phytyl-/steryl-esters during nitrogen starvation

To determine the origin of the neutral lipids accumulated in plastoglobules and LDs during senescence, we induced artificial senescence by growing Arabidopsis seedlings on nitrogen-deprived medium (Fig. 6A) and monitored glycerolipid metabolism by radioactive labeling.

For the pulse-chase experiment, 2-week-old Arabidopsis seedlings were first fed with radioactive [^{14}C]acetate for 2 hours and then nitrogen starved for 10 days. Prior to radioactivity quantification, lipids were separated by TLC using a protocol that did not allow phytyl-esters to be separated from SEs. All polar glycerolipids except DGDGs, which are mainly synthesized after an import of lipids from the ER (Browse et al., 1986), were initially labeled, with most of the radioactivity incorporated into MGDG, PC and PG (42, 27 and 13%, respectively; Fig. 6G and Table S1). In contrast, neutral lipids were barely radiolabeled, with only 1.3, 0.4 and 0.2% of the total radioactivity in FFAs, TAGs and phytyl-/steryl-esters, respectively (Table S1).

After 10 days of nitrogen starvation, MGDG radiolabeling decreased from 42% to 35% of total radioactivity, while it remained stable in the seedlings grown on a nitrogen-balanced medium. These results reflect the remobilization of MGDG during nitrogen starvation. The incorporation of the radiolabel into DGDG over the 10-day period was similar in both starved and well-fed plantlets, demonstrating that this incorporation was not linked to induced senescence but rather derived from standard DGDG metabolism, which was apparently unaffected by starvation. At the same time, radioactivity was incorporated into TAGs and phytyl-/steryl-esters at a higher rate in starved plantlets than in supplemented ones (8.9% and 9.3% incorporation of the total radioactivity in starved plantlets versus 0.3% and 5.3% in control plantlets, in TAGs and phytyl-/steryl-esters, respectively, Fig. 6G). This confirmed that TAGs and phytyl-/steryl-esters were synthesized in response to nitrogen starvation but also demonstrated that their synthesis involved, at least in part, the incorporation of

FAs previously constituting other lipids rather than *de novo* synthesized FAs. MGDG is the lipid showing the fastest and greatest loss of radioactive labeling, while the labeling of other polar lipids is more or less similar between starved and supplemented plantlets (Fig. 6G and Table S1). This indicates the incorporation of MGDG-derived FAs into TAGs and phytyl-/steryl-esters during senescence. In addition, during MGDG degradation, no increase in the radiolabel of FFAs was observed, with a remarkably low level of radiolabeled FFAs throughout the kinetics (Table S1), suggesting that no MGDG-derived FAs accumulated as FFAs in the leaf.

In parallel, the glycerolipid distribution and composition of the nitrogen-starved plantlets were also determined (Fig. 7). As observed in naturally aging plants, the relative MGDG content in N-starved plantlets decreased considerably, but its FA composition remained stable and comparable between the starved and control plantlets (Fig. S4). At the same time, the relative DGDG content increased during starvation, while the relative phospholipid content was stable and similar in the starved and control plantlets. The TAG and phytyl-/steryl-ester content increased significantly in response to nitrogen deprivation, with an accumulation of C16:3 in phytyl-/steryl-esters and C18:3 in TAGs, both at the expense of saturated FAs. Overall, these results indicate that, during natural or artificially induced senescence, MGDG degradation releases C16:3 and C18:3 FAs, which are incorporated into neutral lipids accumulating in LDs and plastoglobules.

In agreement with these results, TEM observations revealed that after 10 days of nitrogen starvation, the cross-sectional area of the plastoglobules increased from *ca.* 0.003 μm^2 (or 60 nm in diameter) to *ca.* 0.034 μm^2 (210 nm in diameter). In addition, cytosolic LDs were not observed in parenchyma cells before the starvation period (based on the observation of 40 cells) but accumulated to reach a maximum of 0.013 LD per μm^2 of cell surface with an average LD cross-sectional area of 0.63 μm^2 (Fig. 6B–E). As described in Gaude et al. (2007), the chloroplast ultrastructure was seriously disrupted, with disorganized grana and a dramatic accumulation of starch granules distorting the thylakoid network.

To further elucidate the origin of FAs used for neutral lipid synthesis, the FA composition of TAGs and phytyl-/steryl-esters was determined in *fad2* mutant seedlings before and after 10 days of nitrogen starvation. *fad2* mutant is deficient in the ER-localized desaturase that is responsible for the C18:1 to C18:2 desaturation of ER phospholipids, and displays reduced amount of C18:3 and C18:2 but increased amount of C18:1 mainly in extraplastidic polar lipids, compared to the wild-type (Miquel and Browse, 1992, and Fig. S5). Phytyl-/steryl-esters in *fad2* mutant were enriched in C18:1 and impoverished in C18:2 compared to wild-type, both before and after nitrogen starvation (Fig. 8A), but contained C18:3 in amount similar to wild-type (49 *vs* 43% before starvation and 45 *vs* 41 % after

nitrogen starvation in *fad2* and *Col0* respectively), suggesting that both ER- and plastid-derived FAs contribute to phytyl-/steryl-ester synthesis.

Before nitrogen starvation, TAGs in *fad2* mutant contained 5 times more C18:1 levels than wild type (Fig. 8B), but no C18:2 and very few C18:3 (less than 4% of total FAs), suggesting that FAs contributing to basal TAG synthesis are mainly ER-derived. After 10 days of nitrogen starvation, C18:1 content decreased both in wild type and *fad2* TAGs, but was still 10 times higher in *fad2* mutant than in wild-type. In parallel, C18:3 content increased both in wild-type and *fad2* TAGs after nitrogen starvation to reach 59 and 49% of fatty acids, respectively. This indicates that some FAs desaturated in PCs by FAD2 are incorporated under nitrogen starvation into TAGs, but that the C18:3 present in starvation-induced TAGs mainly derived from chloroplastic lipids.

Neutral lipids are remobilized during repletion

The fate of neutral lipids accumulated in leaf plastoglobules and LDs is still unclear. They could represent a stock of energy, as described in seeds or a pool of FAs directly available for *de novo* membrane biogenesis or membrane remodeling when environmental conditions improve, as described for pollen tube growth (Hernández et al., 2020; Ischebeck, 2016; Mellema et al., 2002). To address this point, nitrogen-starved plantlets were transferred back to nitrogen-balanced media for a further 10 days, and cell ultrastructure, lipid radiolabeling and lipid content were monitored (Figs. 6 and 7). The size of plastoglobules in starved plantlets decreased from *ca.* 0.034 μm^2 cross-sectional area to *ca.* 0.021 μm^2 after 10 days of repletion, which was smaller than that in non-starved plantlets (*ca.* 0.062 μm^2*;* Fig. 6C). Indeed, the size of plastoglobules in control plantlets gradually increased during *in vitro* plant growth, and LDs progressively enlarged in the old control plants (Fig. 6E). This suggests that after 35 days of *in vitro* growth, plantlets suffer stress even on nitrogen-balanced media, which may be due to limited space, gas exchange or light provided by *in vitro* culture (Matuszkiewicz et al., 2019). During the repletion period, the size and number of LDs in parenchyma cells of starved plantlets progressively decreased, and the number of LDs reached a level equivalent to that in control plants (Fig. 6E and F), demonstrating an important remobilization of LDs during the recovery phase. At the same time, the total neutral lipid content in starved plantlets also decreased, from over 16% to less than 7% of total FAs during repletion. The TAGs disappeared completely, while the phytyl-/steryl-ester content remained stable during reversion (Fig. 7A). However, the composition of phytyl-/steryl-esters varied, with a decrease in C16:3 FA and the maintenance of C18:3 (Fig. 7B), suggesting that during repletion, phytyl-esters were remobilized, while SEs were not. Meanwhile, the MGDG content of starved plants gradually increased from 26% to 36%, reaching the MGDG content of the non-starved plants (Fig. 7A).

461 Radiolabeling in TAGs rapidly decreased from 9.0% (±1.4) to 1.6% (±0.6) of total labeling during
462 recovery (Fig. 6G), while labeling rapidly increased in PC from 4.4% (±0.3) to 12.7% (±0.7) after 3 days
463 of recovery and later in MGDG and DGDG (from 32% and 20% at 7 days of recovery to 39% and 25%
464 after 10 days of recovery, respectively, Fig. 6G), suggesting that FAs stored in TAGs are at least
465 partially mobilized for membrane biogenesis when optimal growth conditions are restored. In
466 contrast, phytyl-/steryl-ester labeling did not significantly decrease during the reversion period,
467 confirming that FAs esterified to sterol moieties were mobilized neither for membrane biogenesis
468 nor for energy production, at least during the first 10 days of the recovery phase.
469
470 **LD/plastid contact sites probably facilitate lipid exchange between plastids and LDs**

471 Our results suggest that FAs derived from MGDG degradation in thylakoids are stored in both
472 plastoglobules and cytosolic LDs. The exchange of molecules between thylakoids and plastoglobules
473 probably takes place via the physical channel between thylakoids and plastoglobules created by the
474 outer leaflet of the thylakoid membrane surrounding the plastoglobules (Austin et al., 2006). MGDG-
475 derived FAs could then transit through this channel to be stored in the plastoglobules. The process by
476 which plastid lipids transit to LDs is less evident. However, using TEM, we frequently observed "close
477 proximity" between plastids and LDs, with either no observable space between the two organelles,
478 or a space smaller than that separating the two membranes of the chloroplast envelope (Fig. 9A). In
479 parenchyma cells of plantlets subjected to nitrogen starvation for 7 days, 62% of LDs, on a total of 85
480 images comprising 302 LDs, were observed in close proximity to at least one chloroplast. In
481 comparison, the frequency of LDs in contact with the plasma membrane was estimated at 18% and
482 with mitochondria at 4%. The size of the zone of proximity between the LD and the plastid averaged
483 416±119 nm (out of 60 measured contact sites), meaning that 20.2±6.2% of the perimeter of an LD
484 section was engaged in close contact with chloroplasts. In addition, the morphology of some of the
485 proximity zones between LDs and plastids suggest that these are not "accidental" contacts due to the
486 congestion of the cytoplasm by the large vacuole but rather true areas of metabolite transfer, with a
487 change in the curvature of the droplet, which appears to maximize the area of contact with the
488 plastid (see, for example, middle panel in Fig. 9A).

489 To examine the three-dimensional architecture of these putative plastid–LD contact sites, we
490 performed electron tomography. Single-axis tomograms of the contact zone between LDs and the
491 chloroplast were collected from chemically fixed Arabidopsis leaves (Fig. 9B–D). Modeling of
492 reconstructed tomograms revealed a narrow apposition of the chloroplast envelope to the LD leaflet
493 over a length of around 400 nm, confirming measurements made on classic electron microscopy
494 images. In small parts of this zone of close proximity, the LD appeared to be in physical contact with

the plastid, leaving no apparent gap between the two organelles, while in other parts of the same zone, an intermediate gap of around 4 nm between the LD and the plastid envelope was observed. When close apposition between LD and chloroplast was observed, the outer and inner membranes of the chloroplast envelope appeared closer to each other than anywhere else, as if pressed together, suggesting the presence of a physical factor that favors tight contact between the inner and outer chloroplast membranes on one side and the LD leaflet on the other side.

Discussion:

In this study, we demonstrated that galactolipids are genuine lipids of the plastoglobule monolayer. The presence of MGDG with a high ratio of MGDG/DGDG in plastoglobules compared to thylakoids is surprising because, due to its unsaturated acyl chains, the shape of MGDG is that of an inverted cone, which theoretically favors the formation of a negative curvature rather than the positive one needed to form plastoglobules (Graham Shipley et al., 1973). However, as stated by Simidjiev et al. (2000) "lipid–protein interactions play a major part in imposing a (…) configuration in the native membranes." For example, the CURT1 protein is necessary to induce thylakoid curvature at the grana of Arabidopsis chloroplasts (Armbruster et al., 2013), and the addition of the Light-Harvesting Complex II protein to an MGDG mixture dispersed in water modifies the MGDG organization from an inverted hexagonal (HII) phase to a lamellar structure (Simidjiev et al., 2000). Thus, we hypothesized that plastoglobule proteins, such as fibrillins, the main structural proteins found in plastoglobules, favor the formation of plastoglobules. Moreover, the presence and nature of neutral lipids within the plastoglobules may also favor their formation, as described for LDs (Chorlay and Thiam, 2018; Santinho et al., 2021), where the surface tension generated by neutral lipids within the ER membrane favors the budding of LDs. An enrichment in the plastoglobule monolayer of lyso-galactolipids, with their conical shape, could favor the formation of plastoglobules, but only traces of lyso-galactolipids, equivalent to that in thylakoids, were detected in plastoglobules (Fig. 5C). Additional biophysical studies devoted to plastoglobules are undeniably needed to understand the mechanisms of plastoglobule biogenesis.

The aim of this study was to decipher the interrelations between the two sites of neutral lipid storage in Arabidopsis cells: cytosolic LDs and plastoglobules. We showed that in aging leaves, neutral lipids were stored both in plastoglobules and in cytosolic LDs but that each compartment accumulated different lipids (Figures 3, 4 and 5). Our results demonstrated that, in senescent leaves, the main neutral lipids stored in plastoglobules were, in addition to prenyl quinones, phytyl-esters. Plastoglobules are often viewed as containing a substantial amount of TAGs (Kaup et al., 2002;

Lippold et al., 2012; Rottet et al., 2015; van Wijk and Kessler, 2017), but the genuine presence of triglycerides in this compartment has been called into question in the review written by Lichtenthaler (2013), who found only a limited amount of TAGs in the plastoglobule fractions obtained from *Ficus elastica* and *Tilia* chloroplasts. In this review, Lichtenthaler suggested that the TAGs detected by Tevini and Steinmuller (Steinmüller and Tevini, 1985; Tevini and Steinmüller, 1985) in chloroplasts originated from contamination by cytosolic LDs. Similarly, we found only a limited amount of TAGs (less than 2%mol) in plastoglobules from senescent Arabidopsis leaves (Fig. 3), but the FA composition of the plastoglobule TAGs differed from the LD ones, which excludes possible contamination by cytosolic LDs and argues for a genuine presence, although in a scant amount, of TAGs in plastoglobules. However, larger amounts of TAGs are likely stored within plastoglobules from chromoplasts or etioplasts, for example (Dahlin and Ryberg, 1986; Hansmann and Sitte, 1982; Liu et al., 2024; Steinmüller and Tevini, 1985). In agreement with Mueller *et al*. (2015), who described an extra-chloroplastic accumulation of TAGs in Arabidopsis leaves in response to heat stress, our results demonstrated that cytosolic LDs were the main compartment for TAG storage in senescent leaves. Given that various abiotic stressors lead to the formation of LDs (Ischebeck et al., 2020; Vries and Ischebeck, 2020, and this study), it is probable that TAGs accumulated in response to these environmental changes are stored within cytosolic LDs and that plastoglobules play only a limited or transient role in this storage. Plastids have the capacity to synthesize TAGs (Kaup et al., 2002; Lippold et al., 2012; Martin and Wilson, 1984), and this synthesis either leads to the formation of transient TAGs that do not accumulate within chloroplasts or occurs under very specific developmental stages (such as in etioplasts or chromoplasts) or environmental stress.

It has been proposed that during senescence or different abiotic stress conditions, TAGs are not formed from neo-synthesized FAs but rather represent intermediaries of lipid catabolism, assembled with the FAs released by the degradation of the chloroplast membranes (Cohen et al., 2022; Domínguez and Cejudo, 2021; Kaup et al., 2002; Sakaki et al., 1990). Fan et al. (2017) suggested that upon dark treatment, the accumulating TAG was derived mostly from MGDG and DGDG and that the hydrolyzed MGDG was not converted to DAG before export from the chloroplast, but rather hydrolyzed by lipases to release FFAs that were then exported to the ER. In *Chlamydomonas reinhardtii,* Young and Shachar-Hill (2021) showed that in response to nitrogen starvation, FAs derived from polar lipids were incorporated into TAGs and that the FA moieties coming from the TAGs were used to synthesize new membrane lipids during recovery. The lipid composition of LDs and plastoglobules, together with our labeling experiments demonstrated that at least some of the FAs released by the degradation of MGDG during senescence or nitrogen starvation were incorporated into TAGs and phytyl-/steryl-esters. This was confirmed by the analysis of the TAG and

phytyl-/steryl-ester composition of *fad2* mutant after nitrogen starvation, which indicates that some C18:3 of chloroplastic origin are incorporated in starvation-induced TAGs and phytyl-/steryl-esters (Fig. 8). Similar results were obtained by Mueller et al. (2017) for heat-induced TAGs. Overall, these results establish that during nitrogen starvation, the C16:3 released by MGDG degradation remains within plastids, mainly esterified as phytyl-esters in plastoglobules, while MGDG-released C18:3 is exported outside plastids into LDs and amasses as TAGs and SEs. This suggests the existence of a segregation process taking place at the plastid envelope during senescence or nitrogen starvation, allowing for the export of C18:3 but not C16:3. To our knowledge, the mechanism responsible for and the reasons for such segregation are unknown. The release of FAs from MGDG may involve lipases, such as Arabidopsis PLASTID LIPASE2 (PLIP2) and HEAT INDUCED LIPASE1 (HIL1) (Higashi et al., 2018; Wang et al., 2018). Under heat stress, HIL1 is responsible for the release of C18:3 at the sn-1 position of MGDG, and less 54:9-TAG (corresponding to 18:3-18:3-18:3 TAG) accumulates in heat-stressed leaves of the *hil1* mutant compared to the wild type. This suggests the incorporation of the C18:3 released by HIL1 from MGDG into TAGs, possibly through the intermediary synthesis of phospholipids (Higashi et al., 2018). Similarly, PLIP2 has also been shown to cleave sn-1 C18:3 from MGDG preferentially (Wang et al., 2018) in response to ABA and possibly to different abiotic stressors. The released C18:3 is then used to produce jasmonate. It would be interesting to determine whether at least one of these galactolipases is also activated during senescence or under nitrogen starvation and could participate in MGDG degradation. In this hypothesis, the C18:3 at the sn-1 position is released, exported outside of the plastid and imported in the ER, probably thanks to FA transporters, such as FATTY ACID EXPORT 1 (FAX1) at the plastid envelope (Li et al., 2015) and AtABCA9 transporter at the ER (Kim et al., 2013), and finally incorporated into TAGs or SEs stored within cytosolic LDs as described for TAGs by Tjellström et al. (2015). The fate of the lyso-MGDG remaining in the plastid is unknown. It could be hydrolyzed by a lipase to provide C16:3 that is further incorporated into phytyl-esters by the PHYTYL-ESTER SYNTHASEs PES1 and/or PES2. Another possibility is that lyso-MGDG is directly used as a substrate by PES enzymes, but it remains to be determined whether PES enzymes also accept lyso-MGDG as an acyl donor. Whether other lipases, such as the galactolipid galactosyltransferase SENSITIVE TO FREEZING 2 (SFR2), which catalyzes the formation of DAG and consequently TAG (Moellering et al., 2010), the NPC6 (Nonspecific phospholipase C6) that has been shown to promote galactolipid turnover to TAG production in developing Arabidopsis seeds (Cai et al., 2020), or enzymes with galactosyl hydrolase activity, such as the LD localized CrGH from *C. reinhardtii* (Gu et al., 2021), also participate in the degradation of MGDG and formation of TAGs in response to nitrogen starvation, still needs to be examined.

Surprisingly, we also identified SEs in plastoglobules. SEs are generally described as being associated with cytosolic LDs; thus, their presence in plastoglobules suggests contamination of the plastoglobule

fractions by LDs. However, the specific composition of the SEs found in plastoglobules, compared to those in LDs (Fig. 4C), excludes any contamination of the plastoglobule fraction by LDs. To exclude any contamination by lipids co-migrating with the SEs in the TLC, we performed LC-MS and unambiguously identified SEs in the plastoglobules (Fig. 4D). SEs have already been described in the elaioplasts of *Brassica napus* anthers (Hernández-Pinzón et al., 1999) and more recently C18:2- and C18:3-sitosterols have also been identified in chromoplast plastoglobules of *Citrus sinensis* (Liu et al., 2024). However, the presence of SEs in plastids is unexplained. Their FA composition, enriched notably in the typically plastidial FAs C16:3 and C18:3, suggests that they are synthesized within the plastids rather than imported. This implies that some sterols are esterified by an unidentified plastid esterase putatively the PES enzymes that were shown to synthesize SEs when expressed in a mutant yeast strain lacking TAG and SE synthesis activity (Lippold et al., 2012). Some sterols have indeed been detected in plastid membranes (Hartmann and Benveniste, 1987) and the import of sterols in elaioplasts has also been suggested by Kobayashi *et al*. (2018). The mechanisms allowing the transport of sterols, from one organelle to another, are still unknown. The import of lipids to plastids occurs mainly through non-vesicular pathways and is believed to occur in part via membrane contact sites (Michaud and Jouhet, 2019). Sterols could also transit from the ER to plastids via contact sites, as ER was observed wrapped around and physically associated with the plastids (reviewed in Bian et al., 2023), or through any other membrane contact site involving a sterol-containing membrane.

In *C. reinhardtii*, a physical connection between cytosolic LDs, ER membranes and chloroplasts has been described that likely favors the diffusion of neutral lipids between the ER and plastids through LDs (Goodson et al., 2011; Moriyama et al., 2018). Because we observed frequent apposition of LDs to plastids during nitrogen starvation, we hypothesized that direct transport of lipids from plastids to LDs may occur. Our electron tomography study reinforced this premise by showing that both plastid envelope membranes are closely appressed against each other at the site of LD–plastid contact (Fig. 9), which certainly facilitates lipid channeling between plastids and LDs. The fact that the outer and inner envelope membranes are in close proximity at the LD contact site may explain how TGD2 (TRIGALACTOSYLTRIACYLGLYCEROL-2), a lipid transporter protein located at the inner membrane of the plastid envelope, can be detected in the LD proteomes of Arabidopsis leaves and *C. reinhardtii* (Brocard et al., 2017; Nguyen et al., 2011). We also identified small amounts of galactolipids in LD-enriched fractions, suggesting an export of galactolipids across the plastid envelope to LDs. Such export has already been described during phosphate starvation, where galactolipids replace at least part of the phospholipids in the plastids but also in extraplastidic membranes (Härtel et al., 2000; Klaus et al., 2002) and was suggested to occur through physical contact sites between plastids and mitochondria (Jouhet et al., 2004).

Further structural studies of LD–plastid contact sites will certainly provide more precision about the configuration and functionality of such structures: do these sites of proximity engage hemifusion events between both organelles, as suggested to occur between plastid and ER (Mehrshahi et al., 2013; Mehrshahi et al., 2014), or rather membrane contact sites? Are some stabilizing or tethering elements involved to maintain these sites of proximity and which ones? Do LD–plastid contacts also occur under other stress conditions? When and how are they established? Could leaf LDs occasionally originate from the plastid envelope, as proposed for *C. reinhardtii* (Fan et al., 2011; Tsai et al., 2015)?

The degradation of seed LDs during seed germination has been well described (D'Andrea, 2016; Deruyffelaere et al., 2015; Deruyffelaere et al., 2018; Kelly et al., 2011), but how stress-induced LDs are degraded and contribute to cell homeostasis after returning to normal growth conditions in higher plants remains elusive. Lipids stored in LDs can be degraded by two distinct pathways, namely lipolysis, which relies on the action of lipases, and lipophagy, which refers to the autophagic degradation of LDs in the vacuole (recently reviewed in Bouchnak et al., 2023). It has been demonstrated that both lipolysis and autophagic pathways are involved in TAG remobilization under extended darkness (Fan et al., 2017; Fan et al., 2019). Our study showed that LDs induced by nitrogen starvation disappeared after 10 days of repletion and that TAGs were also fully remobilized, while lipid esters (phytyl- and/or steryl-esters) were not. This suggests the existence of TAG-specific remobilization pathways. Currently, the pathway(s) of neutral lipid remobilization, the fate(s) of TAG-derived FAs and their role in plant recovery are still poorly grasped, and certainly deserve further studies.

Acknowledgments

Lipidomic analyses were performed on the Bordeaux Metabolome Facility-MetaboHUB (ANR-11-INBS-0010) and on the LIPANG (Lipid analysis in Grenoble) hosted by the LPCV (UMR 5168 CNRS-CEA-INRAE-UGA) and supported by the Rhône-Alpes Region, the fonds FEDER, and GRAL, financed within the University Grenoble Alpes graduate school (Ecoles Universitaires de Recherche) CBH-EUR-GS (ANR-17-EURE-0003). Imaging was performed at the Plant imagery facility (PIV), an entity of the Bordeaux Imaging Center (BIC), part of the National Infrastructure France-BioImaging supported by the French National Research Agency (ANR-10-INSB-04). Authors sincerely acknowledge Karim Ait-Alouache and Camille Laveissière for their help in funding management, Jennifer Huard for her valuable help in the wash facility, and Pierre van Delft for his help with computers and GC-FID maintenance. H.N. was recipient of a fellowship from the Conseil Régional d'Aquitaine.

Conflict of Interest

The authors declare that the research was conducted in the absence of any commercial or financial relationships that could be construed as a potential conflict of interest.

Funding

This work was partly supported by the French Agency for Research (Agence Nationale de la Recherche, grant number ANR-21-CE20-0013 RecovOil Project). For the purpose of open access, the author has applied a CC-BY public copyright licence to any Author Accepted Manuscript (AAM) version arising from this submission.

Author contributions: DC, JJB and CB designed the research; DB, JJ, and LF performed the lipid LC-MS/MS analyses; DC, HN, and CB performed the experiments and analyzed the data; DC, JJ, JJB, and CB wrote the manuscript.

REFERENCES:

Armbruster, U., Labs, M., Pribil, M., Viola, S., Xu, W., Scharfenberg, M., Hertle, A. P., Rojahn, U., Jensen, P. E., Rappaport, F., et al. (2013). Arabidopsis CURVATURE THYLAKOID1 proteins modify thylakoid architecture by inducing membrane curvature. *Plant Cell* **25**, 2661–2678.

Austin, J. R., Frost, E., Vidi, P. A., Kessler, F. and Staehelin, L. A. (2006). Plastoglobules are lipoprotein subcompartments of the chloroplast that are permanently coupled to thylakoid membranes and contain biosynthetic enzymes. *Plant Cell* **18**, 1693–703.

Bian, J., Su, X., Yuan, X., Zhang, Y., Lin, J. and Li, X. (2023). Endoplasmic reticulum membrane contact sites: cross-talk between membrane-bound organelles in plant cells. *J. Exp. Bot.* **74**, 2956–2967.

Bouchnak, I., Coulon, D., Salis, V., D'Andréa, S. and Bréhélin, C. (2023). Lipid droplets are versatile organelles involved in plant development and plant response to environmental changes. *Front. Plant Sci.* **14**, 1193905.

Bouvier-Navé, P., Berna, A., Noiriel, A., Compagnon, V., Carlsson, A. S., Banas, A., Stymne, S. and Schaller, H. (2010). Involvement of the Phospholipid Sterol Acyltransferase1 in Plant Sterol Homeostasis and Leaf Senescence. *Plant Physiol.* **152**, 107–119.

Bradford, M. M. (1976). A rapid and sensitive method for the quantitation of microgram quantities of protein utilizing the principle of protein-dye binding. *Anal Biochem* **72**, 248–54.

Bréhélin, C. and Kessler, F. (2008). The Plastoglobule: A Bag Full of Lipid Biochemistry Tricks †. *Photochem. Photobiol.* **84**, 1388–1394.

Brocard, L., Immel, F., Coulon, D., Esnay, N., Tuphile, K., Pascal, S., Claverol, S., Fouillen, L., Bessoule, J.-J. and Bréhélin, C. (2017). Proteomic Analysis of Lipid Droplets from Arabidopsis Aging Leaves Brings New Insight into Their Biogenesis and Functions. *Front. Plant Sci.* **8**, 894.

Browse, J., Warwick, N., Somerville, C. R. and Slack, C. R. (1986). Fluxes through the prokaryotic and eukaryotic pathways of lipid synthesis in the '16:3' plant Arabidopsis thaliana. *Biochem. J.* **235**, 25–31.

Buseman, C. M., Tamura, P., Sparks, A. A., Baughman, E. J., Maatta, S., Zhao, J., Roth, M. R., Esch, S. W., Shah, J., Williams, T. D., et al. (2006). Wounding Stimulates the Accumulation of Glycerolipids Containing Oxophytodienoic Acid and Dinor-Oxophytodienoic Acid in Arabidopsis Leaves. *Plant Physiol.* **142**, 28–39.

Busso, D., Delagoutte-Busso, B. and Moras, D. (2005). Construction of a set Gateway-based destination vectors for high-throughput cloning and expression screening in Escherichia coli. *Anal. Biochem.* **343**, 313–321.

Cai, G., Fan, C., Liu, S., Yang, Q., Liu, D., Wu, J., Li, J., Zhou, Y., Guo, L. and Wang, X. (2020). Nonspecific phospholipase C6 increases seed oil production in oilseed Brassicaceae plants. *New Phytol.* **226**, 1055–1073.

Chapman, K. D., Aziz, M., Dyer, J. M. and Mullen, R. T. (2019). Mechanisms of lipid droplet biogenesis. *Biochem. J.* **476**, 1929–1942.

Chorlay, A. and Thiam, A. R. (2018). An Asymmetry in Monolayer Tension Regulates Lipid Droplet Budding Direction. *Biophys. J.* **114**, 631–640.

Cohen, M., Hertweck, K., Itkin, M., Malitsky, S., Dassa, B., Fischer, A. M. and Fluhr, R. (2022). Enhanced proteostasis, lipid remodeling, and nitrogen remobilization define barley flag leaf senescence. *J. Exp. Bot.* **73**, 6816–6837.

Coulon, D. and Bréhélin, C. (2021). Isolation of Plastoglobules for Lipid Analyses. *Methods Mol. Biol. Clifton NJ* **2295**, 321–335.

Coulon, D., Brocard, L., Tuphile, K. and Bréhélin, C. (2020). Arabidopsis LDIP protein locates at a confined area within the lipid droplet surface and favors lipid droplet formation. *Biochimie* **169**, 29–40.

Dahlin, C. and Ryberg, H. (1986). Accumulation of phytoene in plastoglobuli of SAN-9789 (Norflurazon)-treated dark-grown wheat. *Physiol. Plant.* **68**, 39–45.

D'Andrea, S. (2016). Lipid droplet mobilization: The different ways to loosen the purse strings. *Biochimie* **120**, 17–27.

Demé, B., Cataye, C., Block, M. A., Maréchal, E. and Jouhet, J. (2014). Contribution of galactoglycerolipids to the 3-dimensional architecture of thylakoids. *FASEB J.* **28**, 3373–3383.

Deruère, J., Römer, S., d'Harlingue, A., Backhaus, R. A., Kuntz, M. and Camara, B. (1994). Fibril assembly and carotenoid overaccumulation in chromoplasts: a model for supramolecular lipoprotein structures. *Plant Cell* **6**, 119–133.

Deruyffelaere, C., Bouchez, I., Morin, H., Guillot, A., Miquel, M., Froissard, M., Chardot, T. and D'Andrea, S. (2015). Ubiquitin-Mediated Proteasomal Degradation of Oleosins is Involved in Oil Body Mobilization During Post-Germinative Seedling Growth in Arabidopsis. *Plant Cell Physiol.* **56**, 1374–1387.

Deruyffelaere, C., Purkrtova, Z., Bouchez, I., Collet, B., Cacas, J.-L., Chardot, T., Gallois, J.-L. and D'Andrea, S. (2018). PUX10 Is a CDC48A Adaptor Protein That Regulates the Extraction of Ubiquitinated Oleosins from Seed Lipid Droplets in Arabidopsis. *Plant Cell* **30**, 2116–2136.

Domínguez, F. and Cejudo, F. J. (2021). Chloroplast dismantling in leaf senescence. *J. Exp. Bot.* **72**, 5905–5918.

Dormann, P., Hoffmann-Benning, S., Balbo, I. and Benning, C. (1995). Isolation and characterization of an Arabidopsis mutant deficient in the thylakoid lipid digalactosyl diacylglycerol. *Plant Cell* **7**, 1801–10.

Fan, J., Andre, C. and Xu, C. (2011). A chloroplast pathway for the de novo biosynthesis of triacylglycerol in *Chlamydomonas reinhardtii*. *FEBS Lett.* **585**, 1985–1991.

Fan, J., Yu, L. and Xu, C. (2017). A Central Role for Triacylglycerol in Membrane Lipid Breakdown, Fatty Acid *β* -Oxidation, and Plant Survival under Extended Darkness. *Plant Physiol.* **174**, 1517–1530.

Fan, J., Yu, L. and Xu, C. (2019). Dual Role for Autophagy in Lipid Metabolism in Arabidopsis. *Plant Cell* **31**, 1598–1613.

Ferrer, A., Altabella, T., Arró, M. and Boronat, A. (2017). Emerging roles for conjugated sterols in plants. *Prog. Lipid Res.* **67**, 27–37.

Folch, J., Lees, M. and Stanley, G. H. S. (1957). A Simple Method for the Isolation and Purification of Total Lipides from Animal Tissues. *J. Biol. Chem.* **226**, 497–509.

Gaude, N., Bréhélin, C., Tischendorf, G., Kessler, F. and Dörmann, P. (2007). Nitrogen deficiency in Arabidopsis affects galactolipid composition and gene expression and results in accumulation of fatty acid phytyl esters. *Plant J.* **49**, 729–739.

Gidda, S. K., Park, S., Pyc, M., Yurchenko, O., Cai, Y., Wu, P., Andrews, D. W., Chapman, K. D., Dyer, J. M. and Mullen, R. T. (2016). Lipid Droplet-Associated Proteins (LDAPs) Are Required for the Dynamic Regulation of Neutral Lipid Compartmentation in Plant Cells. *Plant Physiol.* **170**, 2052–2071.

Goodson, C., Roth, R., Wang, Z. T. and Goodenough, U. (2011). Structural Correlates of Cytoplasmic and Chloroplast Lipid Body Synthesis in Chlamydomonas reinhardtii and Stimulation of Lipid Body Production with Acetate Boost. *Eukaryot. Cell* **10**, 1592–1606.

Graham Shipley, G., Green, J. P. and Nichols, B. W. (1973). The phase behavior of monogalactosyl, digalactosyl, and sulphoquinovosyl diglycerides. *Biochim. Biophys. Acta BBA - Biomembr.* **311**, 531–544.

Greenwood, A. D., Leech, R. M. and Williams, J. P. (1963). The osmiophilic globules of chloroplasts. I. Osmiophilic globules as a normal component of chloroplasts and their isolation and composition in Vicia faba L. *Biochim Biophys Acta* **78**, 148–162.

Gu, X., Cao, L., Wu, X., Li, Y., Hu, Q. and Han, D. (2021). A Lipid Bodies-Associated Galactosyl Hydrolase Is Involved in Triacylglycerol Biosynthesis and Galactolipid Turnover in the Unicellular Green Alga Chlamydomonas reinhardtii. *Plants* **10**, 675.

Hansmann, P. and Sitte, P. (1982). Composition and molecular structure of chromoplast globules of Viola tricolor. *Plant Cell Rep.* **1**, 111–114.

Härtel, H., Dörmann, P. and Benning, C. (2000). DGD1-independent biosynthesis of extraplastidic galactolipids after phosphate deprivation in Arabidopsis. *Proc. Natl. Acad. Sci.* **97**, 10649–10654.

Hartmann, M.-A. and Benveniste, P. (1987). Plant membrane sterols: Isolation, identification, and biosynthesis. In *Methods in Enzymology*, pp. 632–650. Academic Press.

Henne, W. M. (2023). The (social) lives, deaths, and biophysical phases of lipid droplets. *Curr. Opin. Cell Biol.* **82**, 102178.

Hernández, M. L., Lima-Cabello, E., Alché, J. de D., Martínez-Rivas, J. M. and Castro, A. J. (2020). Lipid Composition and Associated Gene Expression Patterns during Pollen Germination and Pollen Tube Growth in Olive (Olea europaea L.). *Plant Cell Physiol.* **61**, 1348–1364.

Hernández-Pinzón, I., Ross, J. H. E., Barnes, K. A., Damant, A. P. and Murphy, D. J. (1999). Composition and role of tapetal lipid bodies in the biogenesis of the pollen coat of Brassica napus. *Planta* **208**, 588–598.

Higashi, Y., Okazaki, Y., Myouga, F., Shinozaki, K. and Saito, K. (2015). Landscape of the lipidome and transcriptome under heat stress in Arabidopsis thaliana. *Sci. Rep.* **5**, 10533.

Higashi, Y., Okazaki, Y., Takano, K., Myouga, F., Shinozaki, K., Knoch, E., Fukushima, A. and Saito, K. (2018). HEAT INDUCIBLE LIPASE1 Remodels Chloroplastic Monogalactosyldiacylglycerol by Liberating α-Linolenic Acid in Arabidopsis Leaves under Heat Stress. *Plant Cell* **30**, 1887–1905.

Hiltbrunner, A., Bauer, J., Vidi, P. A., Infanger, S., Weibel, P., Hohwy, M. and Kessler, F. (2001). Targeting of an abundant cytosolic form of the protein import receptor at Toc159 to the outer chloroplast membrane. *J Cell Biol* **154**, 309–16.

Höfte, H. and Chrispeels, M. J. (1992). Protein sorting to the vacuolar membrane. *Plant Cell* **4**, 995–1004.

Horn, P. J., Ledbetter, N. R., James, C. N., Hoffman, W. D., Case, C. R., Verbeck, G. F. and Chapman, K. D. (2011). Visualization of Lipid Droplet Composition by Direct Organelle Mass Spectrometry. *J. Biol. Chem.* **286**, 3298–3306.

Ischebeck, T. (2016). Lipids in pollen - They are different. *Biochim. Biophys. Acta* **1861**, 1315–1328.

Ischebeck, T., Krawczyk, H. E., Mullen, R. T., Dyer, J. M. and Chapman, K. D. (2020). Lipid droplets in plants and algae: Distribution, formation, turnover and function. *Semin. Cell Dev. Biol.* **108**, 82–93.

Jarvis, P., Dormann, P., Peto, C. A., Lutes, J., Benning, C. and Chory, J. (2000). Galactolipid deficiency and abnormal chloroplast development in the Arabidopsis MGD synthase 1 mutant. *Proc Natl Acad Sci U A* **97**, 8175–9.

Jouhet, J., Maréchal, E., Baldan, B., Bligny, R., Joyard, J. and Block, M. A. (2004). Phosphate deprivation induces transfer of DGDG galactolipid from chloroplast to mitochondria. *J. Cell Biol.* **167**, 863–874.

Jouhet, J., Lupette, J., Clerc, O., Magneschi, L., Bedhomme, M., Collin, S., Roy, S., Maréchal, E. and Rébeillé, F. (2017). LC-MS/MS versus TLC plus GC methods: Consistency of glycerolipid and fatty acid profiles in microalgae and higher plant cells and effect of a nitrogen starvation. *PLOS ONE* **12**, e0182423.

Juguelin, H., Heape, A., Boiron, F. and Cassagne, C. (1986). A quantitative developmental study of neutral lipids during myelinogenesis in the peripheral nervous system of normal and trembler mice. *Brain Res.* **390**, 249–252.

Kaup, M. T., Froese, C. D. and Thompson, J. E. (2002). A role for diacylglycerol acyltransferase during leaf senescence. *Plant Physiol.* **129**, 1616–1626.

Kelly, A. A., Quettier, A.-L., Shaw, E. and Eastmond, P. J. (2011). Seed storage oil mobilization is important but not essential for germination or seedling establishment in Arabidopsis. *Plant Physiol.* **157**, 866–875.

Kim, S., Yamaoka, Y., Ono, H., Kim, H., Shim, D., Maeshima, M., Martinoia, E., Cahoon, E. B., Nishida, I. and Lee, Y. (2013). AtABCA9 transporter supplies fatty acids for lipid synthesis to the endoplasmic reticulum. *Proc. Natl. Acad. Sci.* **110**, 773–778.

Klaus, D., Härtel, H., Fitzpatrick, L. M., Froehlich, J. E., Hubert, J., Benning, C. and Dörmann, P. (2002). Digalactosyldiacylglycerol Synthesis in Chloroplasts of the Arabidopsis *dgd1* Mutant. *Plant Physiol.* **128**, 885–895.

Kobayashi, K., Suzuki, M., Muranaka, T. and Nagata, N. (2018). The mevalonate pathway but not the methylerythritol phosphate pathway is critical for elaioplast and pollen coat development in *Arabidopsis*. *Plant Biotechnol.* **35**, 381–385.

Lee, H. G., Park, M.-E., Park, B. Y., Kim, H. U. and Seo, P. J. (2019). The Arabidopsis MYB96 Transcription Factor Mediates ABA-Dependent Triacylglycerol Accumulation in Vegetative Tissues under Drought Stress Conditions. *Plants* **8**, 296.

Leggett Bailey, J. and Whyborn, A. G. (1963). The osmiophilic globules of chloroplasts II. Globules of the spinach-beet chloroplast. *Biochim. Biophys. Acta* **78**, 163–174.

Li, N., Gügel, I. L., Giavalisco, P., Zeisler, V., Schreiber, L., Soll, J. and Philippar, K. (2015). FAX1, a Novel Membrane Protein Mediating Plastid Fatty Acid Export. *PLOS Biol.* **13**, e1002053.

Lichtenthaler, H. K. (1968). Plastoglobuli and the fine structure of plastids. *Endeavor* **27**, 144–149.

Lichtenthaler, H. K. (2013). Plastoglobuli, Thylakoids, Chloroplast Structure and Development of Plastids. In *Plastid Development in Leaves during Growth and Senescence* (ed. Biswal, B.), Krupinska, K.), and Biswal, U. C.), pp. 337–361. Dordrecht: Springer Netherlands.

Lin, W. and Oliver, D. J. (2008). Role of triacylglycerols in leaves. *Plant Sci.* **175**, 233–237.

Lippold, F., Dorp, K. vom, Abraham, M., Hölzl, G., Wewer, V., Yilmaz, J. L., Lager, I., Montandon, C., Besagni, C., Kessler, F., et al. (2012). Fatty Acid Phytyl Ester Synthesis in Chloroplasts of Arabidopsis. *Plant Cell* **24**, 2001–2014.

Liu, Y., Ye, J., Zhu, M., Atkinson, R. G., Zhang, Y., Zheng, X., Lu, J., Cao, Z., Peng, J., Shi, C., et al. (2024). Multi-omics analyses reveal the importance of chromoplast plastoglobules in carotenoid accumulation in citrus fruit. *Plant J.* **117**, 924–943.

Lohmann, A., Schöttler, M. A., Bréhélin, C., Kessler, F., Bock, R., Cahoon, E. B. and Dörmann, P. (2006). Deficiency in Phylloquinone (Vitamin K_1) Methylation Affects Prenyl Quinone Distribution, Photosystem I Abundance, and Anthocyanin Accumulation in the *Arabidopsis AtmenG* Mutant. *J. Biol. Chem.* **281**, 40461–40472.

Lu, J., Xu, Y., Wang, J., Singer, S. D. and Chen, G. (2020). The Role of Triacylglycerol in Plant Stress Response. *Plants* **9**, 472.

Martin, B. A. and Wilson, R. F. (1984). Subcellular localization of triacylglycerol synthesis in spinach leaves. *Lipids* **19**, 117–121.

Matuszkiewicz, M., Koter, M. D. and Filipecki, M. (2019). Limited ventilation causes stress and changes in Arabidopsis morphological, physiological and molecular phenotype during in vitro growth. *Plant Physiol. Biochem.* **135**, 554–562.

Mehrshahi, P., Stefano, G., Andaloro, J. M., Brandizzi, F., Froehlich, J. E. and DellaPenna, D. (2013). Transorganellar complementation redefines the biochemical continuity of endoplasmic reticulum and chloroplasts. *Proc. Natl. Acad. Sci. U. S. A.* **110**, 12126–12131.

Mehrshahi, P., Johnny, C. and DellaPenna, D. (2014). Redefining the metabolic continuity of chloroplasts and ER. *Trends Plant Sci.* **19**, 501–507.

Mellema, S., Eichenberger, W., Rawyler, A., Suter, M., Tadege, M. and Kuhlemeier, C. (2002). The ethanolic fermentation pathway supports respiration and lipid biosynthesis in tobacco pollen. *Plant J.* **30**, 329–336.

Michaud, M. and Jouhet, J. (2019). Lipid Trafficking at Membrane Contact Sites During Plant Development and Stress Response. *Front. Plant Sci.* **10**, 2.

Miquel, M. and Browse, J. (1992). Arabidopsis mutants deficient in polyunsaturated fatty acid synthesis. Biochemical and genetic characterization of a plant oleoyl-phosphatidylcholine desaturase. *J. Biol. Chem.* **267**, 1502–1509.

Miwa, T. K. (1971). Jojoba oil wax esters and derived fatty acids and alcohols: Gas chromatographic analyses. *J. Am. Oil Chem. Soc.* **48**, 259–264.

Moellering, E. R., Muthan, B. and Benning, C. (2010). Freezing Tolerance in Plants Requires Lipid Remodeling at the Outer Chloroplast Membrane. *Science* **330**, 226–228.

Morelli, L., Torres-Montilla, S., Glauser, G., Shanmugabalaji, V., Kessler, F. and Rodriguez-Concepcion, M. (2023). Novel insights into the contribution of plastoglobules and reactive oxygen species to chromoplast differentiation. *New Phytol.* **237**, 1696–1710.

Moriyama, T., Toyoshima, M., Saito, M., Wada, H. and Sato, N. (2018). Revisiting the Algal "Chloroplast Lipid Droplet": The Absence of an Entity That Is Unlikely to Exist. *Plant Physiol.* **176**, 1519–1530.

Mueller, S. P., Krause, D. M., Mueller, M. J. and Fekete, A. (2015). Accumulation of extra-chloroplastic triacylglycerols in *Arabidopsis* seedlings during heat acclimation. *J. Exp. Bot.* **66**, 4517–4526.

Mueller, S. P., Unger, M., Guender, L., Fekete, A. and Mueller, M. J. (2017). Phospholipid:Diacylglycerol Acyltransferase-Mediated Triacylglyerol Synthesis Augments Basal Thermotolerance. *Plant Physiol.* **175**, 486–497.

Nguyen, H. M., Baudet, M., Cuiné, S., Adriano, J.-M., Barthe, D., Billon, E., Bruley, C., Beisson, F., Peltier, G., Ferro, M., et al. (2011). Proteomic profiling of oil bodies isolated from the unicellular green microalga Chlamydomonas reinhardtii: With focus on proteins involved in lipid metabolism. *PROTEOMICS* **11**, 4266–4273.

Rensink, W. A., Pilon, M. and Weisbeek, P. (1998). Domains of a transit sequence required for in vivo import in Arabidopsis chloroplasts. *Plant Physiol* **118**, 691–9.

Rottet, S., Besagni, C. and Kessler, F. (2015). The role of plastoglobules in thylakoid lipid remodeling during plant development. *Biochim. Biophys. Acta BBA - Bioenerg.* **1847**, 889–899.

Sakaki, T., Kondo, N. and Yamada, M. (1990). Pathway for the Synthesis of Triacylglycerols from Monogalactosyldiacylglycerols in Ozone-Fumigated Spinach Leaves. *Plant Physiol* **94**, 773–780.

Santinho, A., Chorlay, A., Foret, L. and Thiam, A. R. (2021). Fat inclusions strongly alter membrane mechanics. *Biophys. J.* **120**, 607–617.

Schneider, C. A., Rasband, W. S. and Eliceiri, K. W. (2012). NIH Image to ImageJ: 25 years of image analysis. *Nat. Methods* **9**, 671–675.

Shimada, T. L., Takano, Y., Shimada, T., Fujiwara, M., Fukao, Y., Mori, M., Okazaki, Y., Saito, K., Sasaki, R., Aoki, K., et al. (2014). Leaf oil body functions as a subcellular factory for the production of a phytoalexin in Arabidopsis. *Plant Physiol.* **164**, 105–118.

Shimada, T. L., Takano, Y. and Hara-Nishimura, I. (2015). Oil body-mediated defense against fungi: From tissues to ecology. *Plant Signal. Behav.* **10**, e989036.

Simidjiev, I., Stoylova, S., Amenitsch, H., Javorfi, T., Mustardy, L., Laggner, P. and Holzenburg, A. (2000). Self-assembly of large, ordered lamellae from non-bilayer lipids and integral membrane proteins in vitro. *Proc. Natl. Acad. Sci.* **97**, 1473–1476.

Steinmüller, D. and Tevini, M. (1985). Composition and function of plastoglobuli. I. Isolation and purification from chloroplasts and chromoplasts. *Planta* **163**, 201–207.

Tevini, M. and Steinmüller, D. (1985). Composition and function of plastoglobuli. II. Lipid composition of leaves and plastoglobuli during beech leaf senescence. *Planta* **163**, 91–96.

Tjellström, H., Strawsine, M. and Ohlrogge, J. B. (2015). Tracking synthesis and turnover of triacylglycerol in leaves. *J. Exp. Bot.* **66**, 1453–1461.

Tsai, C.-H., Zienkiewicz, K., Amstutz, C. L., Brink, B. G., Warakanont, J., Roston, R. and Benning, C. (2015). Dynamics of protein and polar lipid recruitment during lipid droplet assembly in *Chlamydomonas reinhardtii*. *Plant J.* **83**, 650–660.

Tzen, Jtc., Cao, Yz., Laurent, P., Ratnayake, C. and Huang, Ahc. (1993). Lipids, Proteins, and Structure of Seed Oil Bodies from Diverse Species. *Plant Physiol.* **101**, 267–276.

Vallon, O., Wollman, F. A. and Olive, J. (1986). Lateral distribution of the main protein complexes of the photosynthetic apparatus in Chlamydomonas reinhardtii and in spinach: an immunocytochemical study using intact thylakoid membranes and a PS II enriched membrane preparation. *Photobiochem. Photobiophys.* **12**, 203–220.

van Wijk, K. J. and Kessler, F. (2017). Plastoglobuli: Plastid Microcompartments with Integrated Functions in Metabolism, Plastid Developmental Transitions, and Environmental Adaptation. *Annu. Rev. Plant Biol.* **68**, 253–289.

Vidi, P.-A., Kanwischer, M., Baginsky, S., Austin, J. R., Csucs, G., Dörmann, P., Kessler, F. and Bréhélin, C. (2006). Tocopherol cyclase (VTE1) localization and vitamin E accumulation in chloroplast plastoglobule lipoprotein particles. *J. Biol. Chem.* **281**, 11225–11234.

Vitiello, F. and Zanetta, J. P. (1978). Thin-layer chromatography of phospholipids. *J. Chromatogr.* **166**, 637–640.

Vries, J. de and Ischebeck, T. (2020). Ties between Stress and Lipid Droplets Pre-date Seeds. *Trends Plant Sci.* **25**, 1203–1214.

Wang, K., Guo, Q., Froehlich, J. E., Hersh, H. L., Zienkiewicz, A., Howe, G. A. and Benning, C. (2018). Two Abscisic Acid-Responsive Plastid Lipase Genes Involved in Jasmonic Acid Biosynthesis in Arabidopsis thaliana. *Plant Cell* **30**, 1006–1022.

Wessel, D. and Flugge, U. I. (1984). A method for the quantitative recovery of protein in dilute solution in the presence of detergents and lipids. *Anal Biochem* **138**, 141–143.

Wu, S. S. H., Platt, K. A., Ratnayake, C., Wang, T.-W., Ting, J. T. L. and Huang, A. H. C. (1997). Isolation and characterization of neutral-lipid-containing organelles and globuli-filled plastids from Brassica napus tapetum. *Proc. Natl. Acad. Sci. U. S. A.* **94**, 12711–12716.

Xu, C. and Shanklin, J. (2016). Triacylglycerol Metabolism, Function, and Accumulation in Plant Vegetative Tissues. *Annu. Rev. Plant Biol.* **67**, 179–206.

Yang, Z. and Ohlrogge, J. B. (2009). Turnover of Fatty Acids during Natural Senescence of Arabidopsis, Brachypodium, and Switchgrass and in Arabidopsis β-Oxidation Mutants. *Plant Physiol.* **150**, 1981–1989.

Young, D. Y. and Shachar-Hill, Y. (2021). Large fluxes of fatty acids from membranes to triacylglycerol and back during N-deprivation and recovery in *Chlamydomonas*. *Plant Physiol.* **185**, 796–814.

Ytterberg, A. J., Peltier, J. B. and van Wijk, K. J. (2006). Protein profiling of plastoglobules in chloroplasts and chromoplasts. A surprising site for differential accumulation of metabolic enzymes. *Plant Physiol* **140**, 984–97.

Yu, C.-W., Lin, Y.-T. and Li, H. (2020). Increased ratio of galactolipid MGDG: DGDG induces jasmonic acid overproduction and changes chloroplast shape. *New Phytol.* **228**, 1327–1335.

Yu, L., Zhou, C., Fan, J., Shanklin, J. and Xu, C. (2021). Mechanisms and functions of membrane lipid remodeling in plants. *Plant J.* **107**, 37–53.

Zbierzak, A. M., Kanwischer, M., Wille, C., Vidi, P.-A., Giavalisco, P., Lohmann, A., Briesen, I., Porfirova, S., Bréhélin, C., Kessler, F., et al. (2009). Intersection of the tocopherol and plastoquinol metabolic pathways at the plastoglobule. *Biochem. J.* **425**, 389–399.

Zhang, C., Qu, Y., Lian, Y., Chapman, M., Chapman, N., Xin, J., Xin, H. and Liu, L. (2020). A new insight into the mechanism for cytosolic lipid droplet degradation in senescent leaves. *Physiol. Plant.* **168**, 835–844.

Zhou, X., Chen, X., Du, Z., Zhang, Y., Zhang, W., Kong, X., Thelen, J. J., Chen, C. and Chen, M. (2019). Terpenoid Esters Are the Major Constituents From Leaf Lipid Droplets of Camellia sinensis. *Front. Plant Sci.* **10**,.

Zienkiewicz, K. and Zienkiewicz, A. (2020). Degradation of Lipid Droplets in Plants and Algae—Right Time, Many Paths, One Goal. *Front. Plant Sci.* **11**, 579019.

Zita, W., Bressoud, S., Glauser, G., Kessler, F. and Shanmugabalaji, V. (2022). Chromoplast plastoglobules recruit the carotenoid biosynthetic pathway and contribute to carotenoid accumulation during tomato fruit maturation. *PloS One* **17**, e0277774.

FIGURE LEGENDS:

Figure 1: Ultrastructure and lipid composition of Arabidopsis leaves at different ages. A. Macroscopic aspect of 6-week-old Arabidopsis plantlets grown at high density; **B.** Ultrastructure of mesophyll cells from 3-week-old (B1), and 6-week-old green (B2), brown (B3) and purple (B4) Arabidopsis leaves. Bar: 5 µm, Chl: chloroplast, St: starch granum, pgl: plastoglobule, LD: lipid droplets; **C.** Quantification of the size and number of plastoglobules and LDs. Values are means ± SD of the number of measures indicated in brackets **D.** Glycerolipids, phytyl- and steryl-esters content in Arabidopsis (Columbia 0) leaves at different ages expressed in µg of fatty acid per mg of fresh weight (FW). Error bars indicate SD of six biological replicates.

Figure 2: Fatty acid distribution of MGDGs, TAGs, phytyl- and steryl-esters in 3- to 6-week-old Arabidopsis leaves. The composition of MGDG (A), TAG (B), phytyl-esterS (C), and steryl-esters (D) was determined by TLC/GC-FID. The provided values are means and SD of six biological replicates.

Figure 3: Neutral lipid composition of Arabidopsis plastoglobules and lipid droplets from 6-week-old leaves. A. Immunoblots of 6-week-old Arabidopsis leaf protein extracts of plastoglobules (PGl), lipid droplets (LD), soluble fraction (Sol.), microsomal fraction (Mic.), total extract (TE), thylakoids (Thyl.) and plastid envelopes (Env.), performed with antibodies raised against plastoglobule (AtFBN1a/AtPGL35), lipid droplet (AtLDAP1), endoplasmic reticulum (Bip), thylakoids (P16) and plastid envelope (Toc75) markers. B. Neutral lipid composition (in %mol) of purified plastoglobules determined by TLC coupled to GC-FID (n=7). C. Neutral lipid composition (in %mol) of lipid droplets determined by TLC coupled to GC-FID (n=5). D. Corrected neutral lipid composition (in %mol) of lipid droplets, after removal of the plastoglobule contaminating lipids. The provided values are means and SD of different biological replicates.

Figure 4: Fatty acid distribution of neutral lipids in plastoglobules and lipid droplets from 6-week-old Arabidopsis leaves. The composition of TAGs (A), phytyl-esters (B) and steryl-esters (C) was determined by GC-FID. The identity of the steryl-esters was also determined by LC-MS/MS (D). The global FA composition (E) of plastoglobules and lipid droplets was calculated based on GC-FID quantifications. Values are means ± SD of 7 (plastoglobules) and 5 (LDs) biological replicates.

Figure 5: Molecular species distribution of DGDG (A) and MGDG (B) from lipid droplets, plastoglobules and thylakoids of 6-week-old Arabidopsis leaves. The composition was determined by LC-MS/MS. Means and SD of 5 (LDs), 7 (plastoglobules) and 10 (thylakoids) biological replicates are shown. ** and *** represent statistically significant differences at p-value ≤ 0.01 and p-value ≤ 0.005, respectively, as determined by Wilcoxon test. C: Repartition of the galactolipids within LD, plastoglobule and thylakoid fractions.

Figure 6: Effects of nitrogen starvation followed by a repletion period on Arabidopsis leaf cell ultrastructure and lipid metabolism. A. Scheme of the experimental procedure showing the labelling pulse of two-week-old plantlets, the 10 days of starvation on nitrogen depleted medium and the recovery phase for 10 supplemental days on nitrogen balanced medium. The control plantlets followed the same experimental procedure excepted that they were always transferred to nitrogen balanced medium. **B.** Ultrastructure of chemically fixed Arabidopsis leaves after 10 days of nitrogen starvation ($10N^-$) or 10 days of controlled growing conditions ($10N^+$) and 10 supplemental days of repletion ($20N^-$ or $20\ N^+$), observed by transmission electron microscopy. Scale bar: 1 µm; Quantification of the size of plastoglobules (**C**., cross-section area, in μm^2), number of plastoglobules per plastid (**D**.), size of LDs (**E**., cross-section area, in μm^2), and number of LDs per cell section area (**F**., μm^{-2}) in response to nitrogen starvation and after repletion. Bar = 1 µm. Pgl: plastoglobules. (more than 40 quantifications per parameter were obtained on at least 2 independent plants). **G.** Kinetics of the radiolabelling of MGDG, DGDG, phytyl-/steryl-esters and TAGs during nitrogen starvation and recovery phases. Grey area corresponds to nitrogen starvation period. Values are means ± SD of five biological replicates.

Figure 7: Glycerolipid analyses of Arabidopsis plantlets during nitrogen starvation and reversion. A. Glycerolipid distribution (in % of lipids); B. Neutral lipid fatty acid content (in µg/mg fresh weight). Two-week-old Arabidopsis plantlets were grown for 10 days on nitrogen balanced medium (N^+) or on nitrogen deprived medium (N^-, grey area) and their lipid composition determined by TLC/GC-FID at day 0 (D0), 3 (D3), 7 (D7) and 10 (D10). Plantlets were then transferred to nitrogen balanced medium for reversion, and their lipid composition similarly monitored after 5 days (D15) and 10 days (D20). Green bars: plantlets grown on nitrogen balanced medium; orange bars: plantlets submitted to nitrogen starvation for 10 days. For clarity reason, values of D0 are presented twice: with control (green) as well as with starved (orange) samples. Values are means ± SD of 4 biological replicates. P-/S-Esters : Phytyl-/Steryl-esters.

Figure 8: Fatty acid composition of neutral lipids from Col0 and *fad2* Arabidopsis plantlets during nitrogen starvation. Two-week-old Arabidopsis plantlets were grown for 10 days on nitrogen

deprived medium and lipid extracted. The fatty acid compositions of phytyl-/steryl-esters (A) and TAGs (B) were determined by TLC/GC-FID before starvation (D0), and after 10 days of starvation (D10 N-). Green bars: *Col0* wild type; blue bars: *fad2* mutant. Values are means ± SD of 4 or 6 biological replicates for *Col0* or *fad2* respectively.

Figure 9: Morphology of the plastid-lipid droplet contact monitored by tomography. The ultrastructure was determined on chemically fixed Arabidopsis leaves subjected for 7 days to nitrogen starvation. A. Electron micrographs showing close proximity (white arrow heads) between LD and chloroplast. Bar: 0.5 µm. **B.** Overview of the contact between a chloroplast and a LD. Bar: 0.5 µm **C.** Tomographic slices of plastid-LD contact site shown in B., highlighting the appression of both plastid envelope membranes with the LD monolayer (white arrow heads). Bar: 0.1 µm. LD: lipid droplet; Env.: plastid envelope; iM: inner membrane of the plastid envelope; oM: outer membrane of the plastid envelope; PG: plastoglobule; Thyl.: thylakoids. The thickness of one tomographic slice is estimated to be around 0.23 nm. **D.** 3D segmentation of C; yellow: LD surface, light pink: outer envelope membrane, purple: inner envelope membrane, green: thylakoids, cream: starch granule.

Figure S1: Fatty acid distribution of phosphatidylcholine (A), phosphatidylinositol (B), phosphatic acid (C), a mix of phosphatidylethanolamine and phosphatidylglycerol (D), and digalactosyldiacylglycerol (E) in leaves from 3- to 6-week-old Arabidopsis plantlets. The fatty acid distribution was determined by TLC/GC-FID. Values are means ± SD of 6 biological replicates.

Figure S2 : LC-MS and GC-FID responses for Steryl Ester analysis

(A) LC-MS analysis of cholesteryl esters. A solution of cholesteryl ester standards, containing equal quantities (in mass) of 18:0-Cholesterol (C79409, Sigma Aldrich, ≥96%), 18:1-Cholesterol (C9253, Sigma Aldrich, ≥98%), and 18:2-Cholesterol (C0289, Sigma Aldrich, ≥98%) was prepared and a volume corresponding to 1.25 pg of each standard was injected and analyzed by LC-MS (MRM). A difference in ionisation yield is observed between the difference SEs, with 18:0-Cholesterol peak aera: 2.464e6, 18:1-Cholesterol peak aera:1.465e7, and 18:2-Cholesterol peak aera:2.95e7 (arbitrary unit).

(B). **GC-FID analysis of the same standard solution.** An aliquot of the cholesteryl ester solution was first transesterified in H_2SO_4 (2,5% v/v) in methanol, containing 5 mg/mL C17:0 as internal standard. After 1h at 85°C, FAMES were extracted using 500µL Hexane and 1 mL H_2O. 1 µL of the hexane phase was injected on GC-FID. Ionisation yield is similar for the different FAMEs, with 18:0 peak area: 1605, 18:1 peak area: 2007, and 18:2 peak area: 2136 (arbitrary unit).

Figure S3: Species distribution of polar lipids in plastoglobules and lipid droplets purified from 6-week-old Arabidopsis leaves, determined by LC-MS. Lipids from plastoglobule, lipid droplet and thylakoid fractions have been extracted and the distribution of species in SQDG (A), phosphatidylglycerol (B), phosphatidylinositol (C) and phosphatidylcholine (D) determined by LC-MS/MS. Means of 3 replicates for lipid droplets and plastoglobules and 5 replicates for thylakoids are shown.

Figure S4: Fatty acid distribution of glycerolipids from Arabidopsis plantlets, during nitrogen starvation and reversion. Two-week-old Arabidopsis plantlets were transferred for 10 days on nitrogen balanced medium or on nitrogen deprived medium (grey area) and their lipid composition determined by TLC/GC-FID at day 0 (D0), 3 (D3), 7 (D7) and 10 (D10). Plantlets were then transferred back to nitrogen balanced medium for reversion, and their lipid composition similarly determined after 5 days (D15) and 10 days (D20). Green bars: plantlets grown on nitrogen balanced medium; orange bars: plantlets submitted to nitrogen starvation for 10 days. For clarity, values of D0 are presented twice: with control (green) as well as with starved (orange) samples. Values represent percents of total FAs, and are means ± SD of 4 biological replicates. FFA: Free Fatty acid, P-/S-Esters : Phytyl-/Steryl-esters.

Figure S5 : Fatty acid composition of PC and MGDG from 2 week old Arabidopsis plantlets. The fatty acid composition of PC (A) and MGDG (B) from Col0 wild type Arabidopsis and *fad2* mutant was determined by TLC/GC-FID after 2 weeks *in vitro* growth on nitrogen-balanced medium. Green bars: wild type Col0; blue bars: *fad2* mutant. Values are means ± SD of 6 biological replicates.

Table S1: Distribution of ^{14}C originating from [^{14}C]acetate among lipids extracted from aerial parts of Arabidopsis plantlets. Two-week-old plantlets were incubated for 2 h with [^{14}C]acetate (time 0), rinsed, and grown *in vitro* on N-balanced (Control plants) or N-deprived (N-starved plants) medium

for 10 days and then transferred on N-balanced medium for recovery during 10 additional days. Samples were harvested at different times during the starvation period (3, 6 and 10 days), and the recovery period (13, 15, 17 and 20 days). All data points are the means ± SD of five biological replicates.

Method S1: LC-MS/MS analyses

A

D

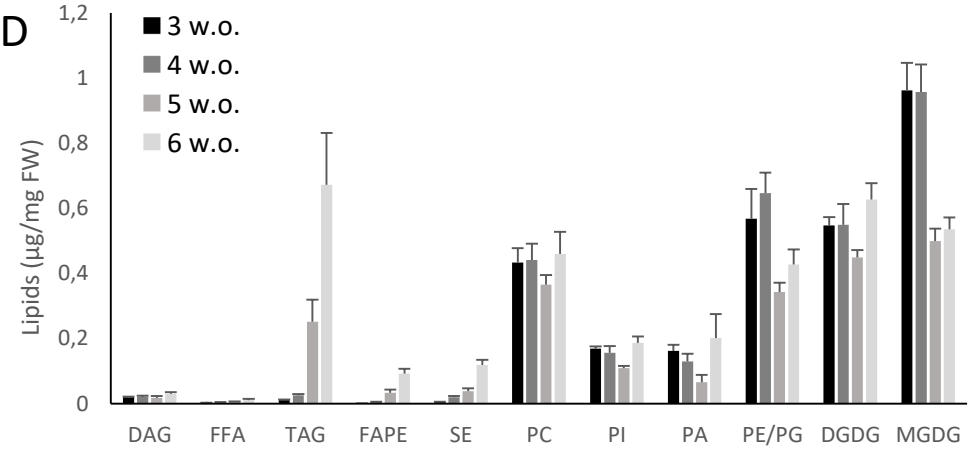

B

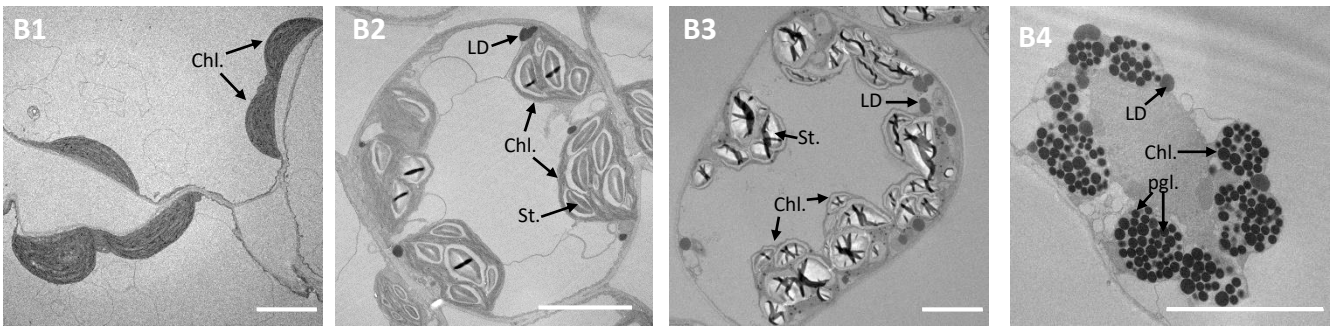

C

	3 w. old	6 w. old
Plastoglobule diameter (nm)	**70 ±14** *(113)*	**226 ±59** *(171)*
LD number per cell cross section	**0.02 ±0.13** *(56)*	**1.27 ±1.53** *(61)*
LD diameter (nm)	*n.d.*	**817 ±251** *(59)*

Figure 1: Ultrastructure and lipid composition of Arabidopsis leaves at different ages. A. Macroscopic aspect of 6-week-old Arabidopsis plantlets grown at high density; **B.** Ultrastructure of mesophyll cells from 3-week-old (B1), and 6-week-old green (B2), brown (B3) and purple (B4) Arabidopsis leaves. Bar: 5 µm, Chl: chloroplast, St: starch granum, pgl: plastoglobule, LD: lipid droplets; **C.** Quantification of the size and number of plastoglobules and LDs. Values are means ± SD of the number of measures indicated in brackets **D.** Glycerolipids, phytyl- and steryl-esters content in Arabidopsis (Columbia 0) leaves at different ages expressed in µg of fatty acid per mg of fresh weight (FW). Error bars indicate SD of six biological replicates.

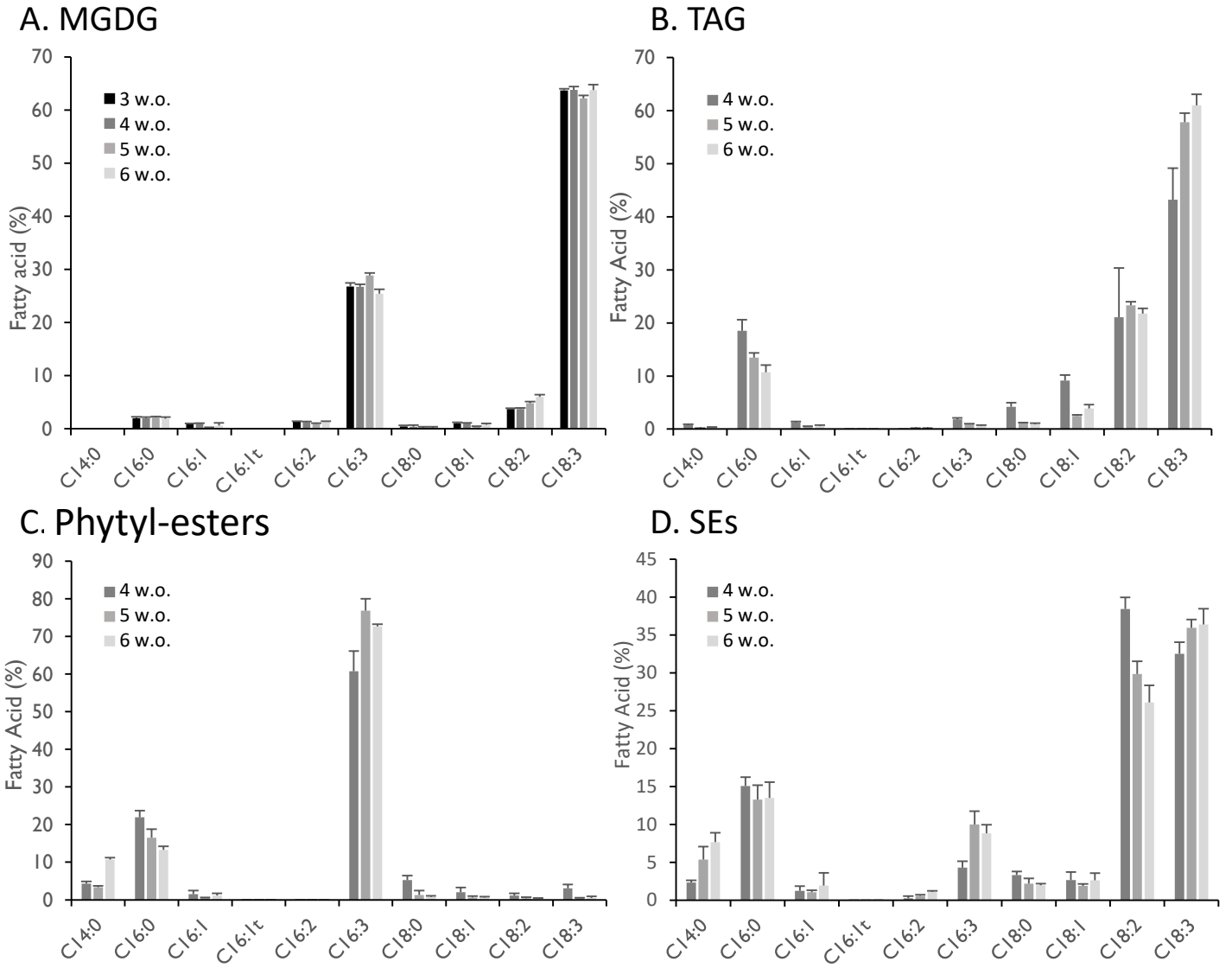

Figure 2: Fatty acid distribution of MGDGs, TAGs, phytyl- and steryl-esters in 3- to 6-week-old Arabidopsis leaves. The composition of each lipid class was determined by TLC/GC-FID. The provided values are means and SD of six biological replicates.

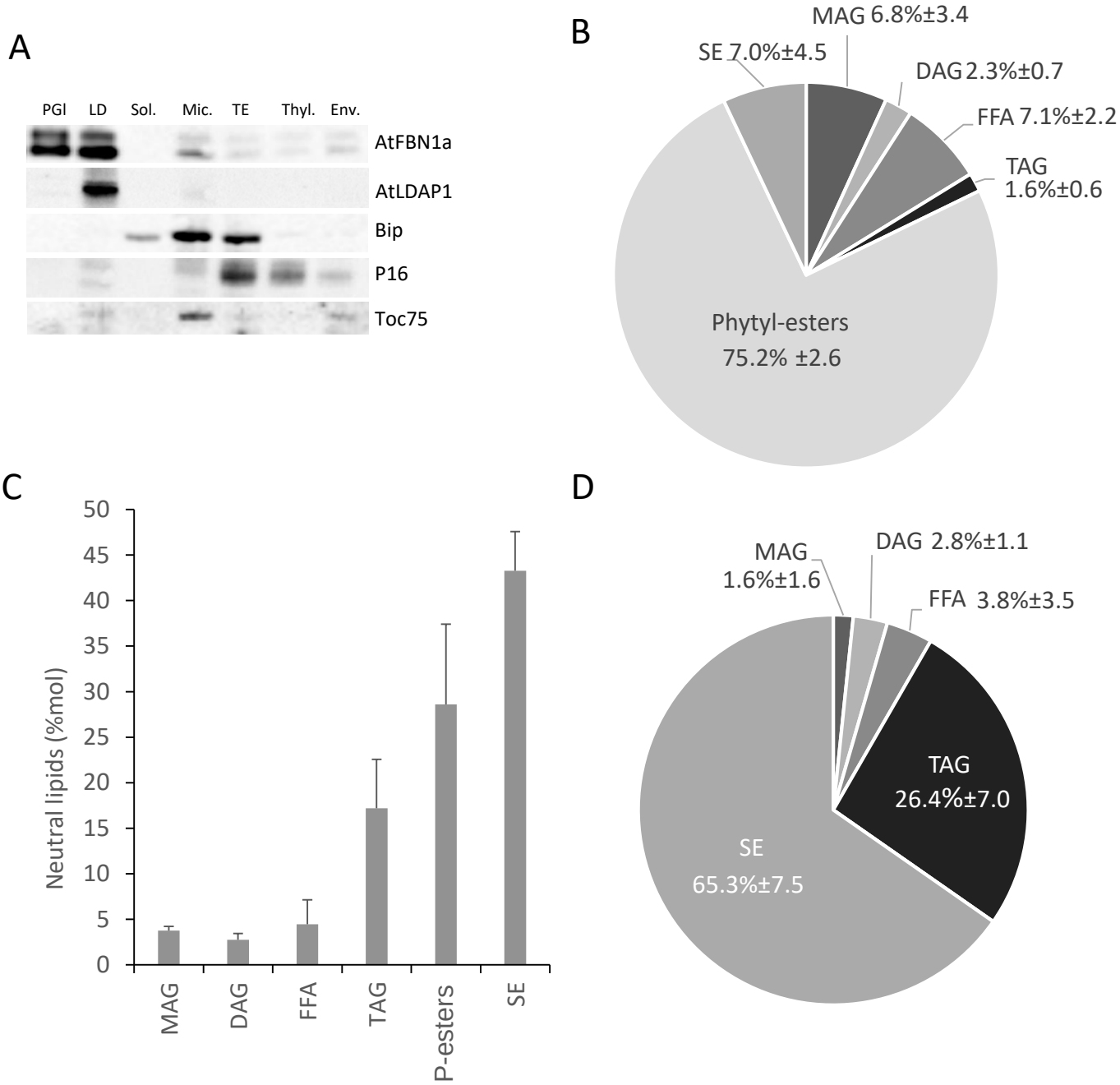

Fig.3: Neutral lipid composition of Arabidopsis plastoglobules and lipid droplets from 6-week-old leaves. A. Immunoblots of 6-week-old Arabidopsis leaf protein extracts of plastoglobules (PGl), lipid droplets (LD), soluble fraction (Sol.), microsomal fraction (Mic.), total extract (TE), thylakoids (Thyl.) and plastid envelopes (Env.), performed with antibodies raised against plastoglobule (AtFBN1a/AtPGL35), lipid droplet (AtLDAP1), endoplasmic reticulum (Bip), thylakoids (P16) and plastid envelope (Toc75) markers. B. Neutral lipid composition (in %mol) of purified plastoglobules determined by TLC coupled to GC-FID (n=7). C. Neutral lipid composition (in %mol) of lipid droplets determined by TLC coupled to GC-FID (n=5). D. Corrected neutral lipid composition (in %mol) of lipid droplets, after removal of the plastoglobule contaminating lipids. The provided values are means and SD of biological replicates. P-esters: Phytyl-esters.

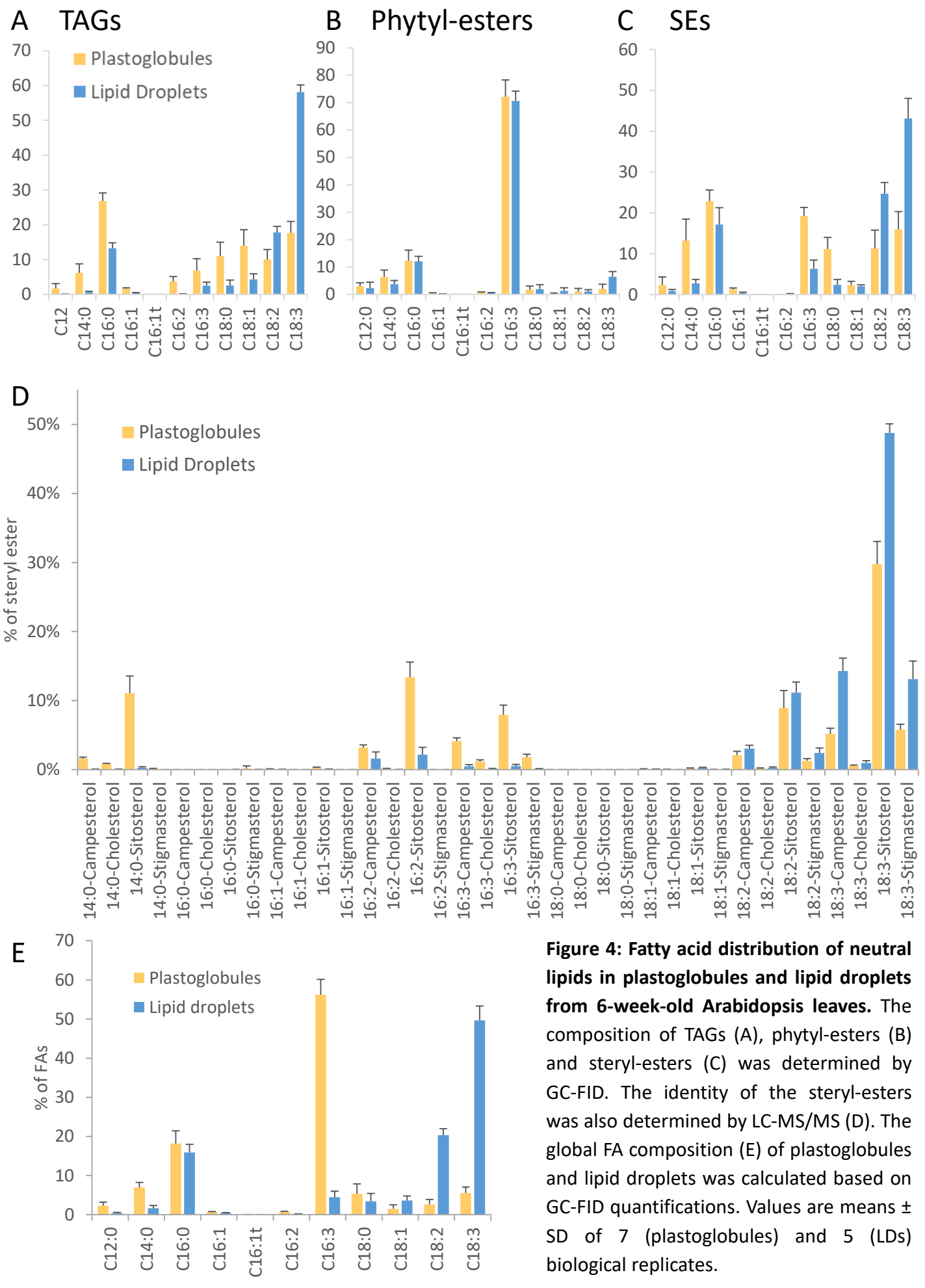

Figure 4: Fatty acid distribution of neutral lipids in plastoglobules and lipid droplets from 6-week-old Arabidopsis leaves. The composition of TAGs (A), phytyl-esters (B) and steryl-esters (C) was determined by GC-FID. The identity of the steryl-esters was also determined by LC-MS/MS (D). The global FA composition (E) of plastoglobules and lipid droplets was calculated based on GC-FID quantifications. Values are means ± SD of 7 (plastoglobules) and 5 (LDs) biological replicates.

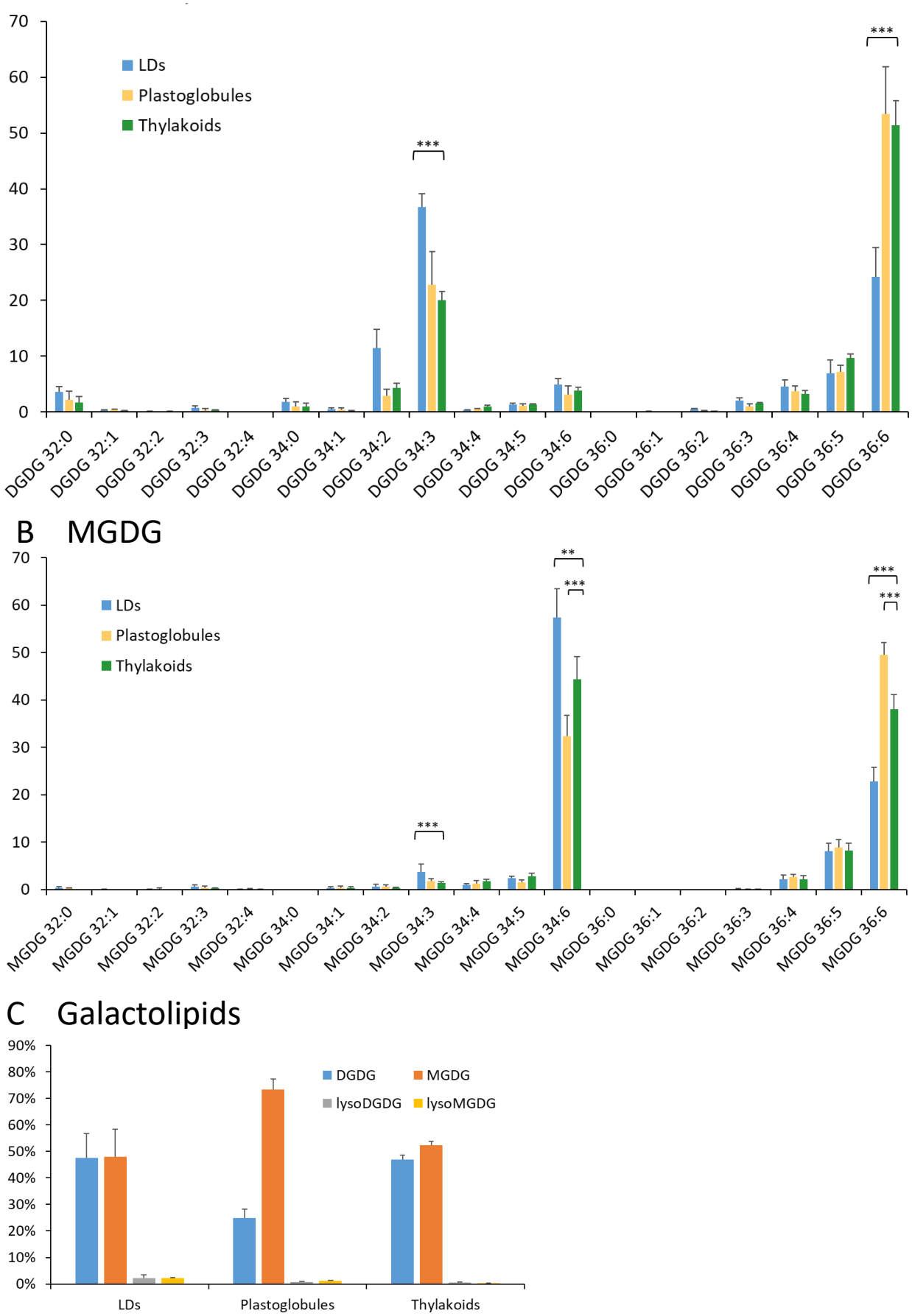

Figure 5: FA distribution of DGDG (A) and MGDG (B) from lipid droplets, plastoglobules and thylakoids of 6-week-old Arabidopsis leaves. The composition was determined by LC-MS/MS. Means and SD of 5 (LDs), 7 (plastoglobules) and 10 (thylakoids) biological replicates are shown. ** and *** represent statistically significant differences at p-value ≤ 0.01 and p-value ≤ 0.005, respectively, as determined by Wilcoxon test. C: Repartition of the galactolipids within LD, plastoglobule and thylakoid fractions.

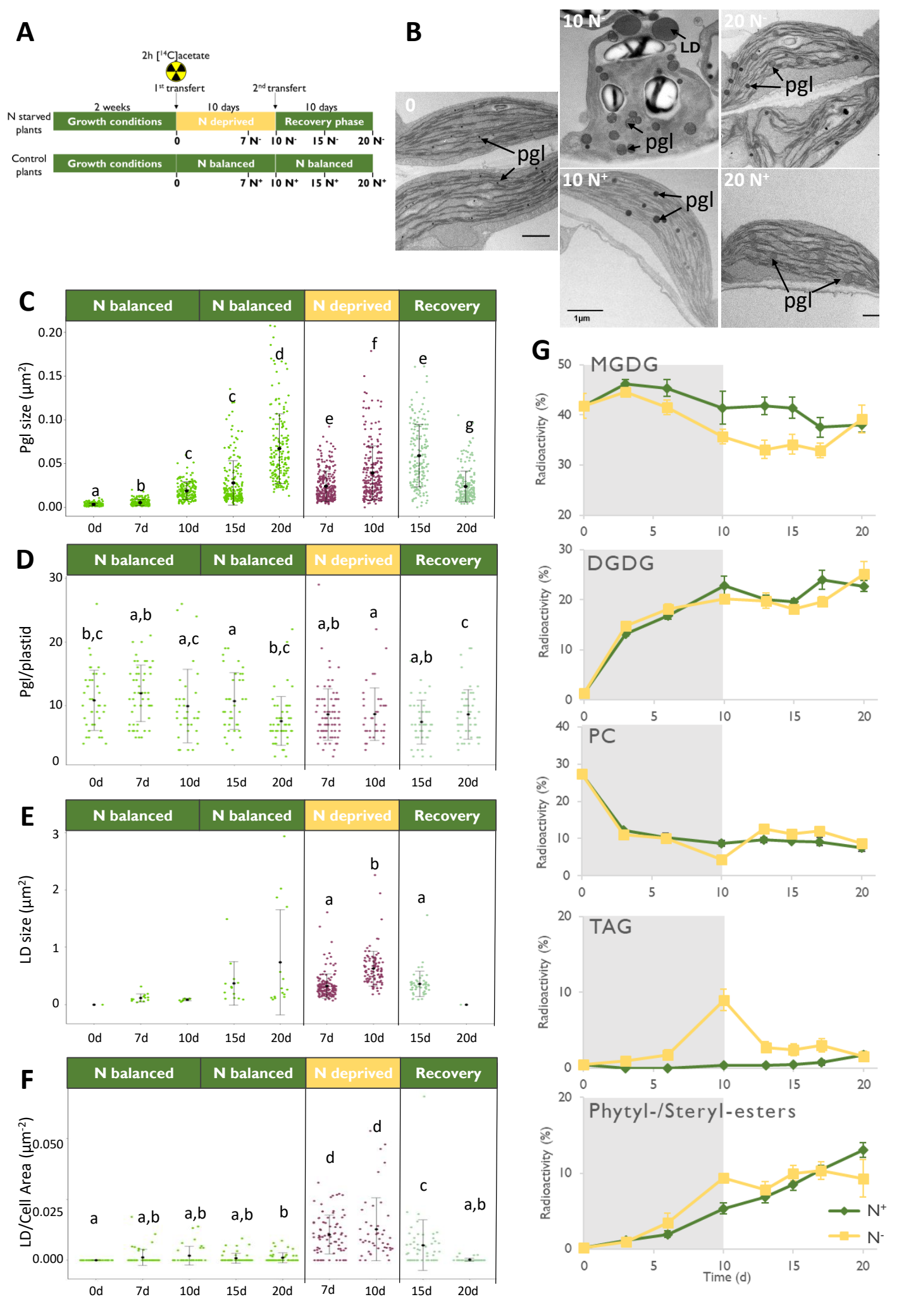
A
2h [14C]acetate
1st transfert
2nd transfert
2 weeks
10 days
10 days
N starved plants
Growth conditions
N deprived
Recovery phase
0
7 N-
10 N-
15 N-
20 N-
Control plants
Growth conditions
N balanced
N balanced
0
7 N+
10 N+
15 N+
20 N+
B
0
pgl
10 N-
LD
pgl
20 N-
pgl
10 N+
pgl
20 N+
pgl
1µm
C
N balanced
N balanced
N deprived
Recovery
Pgl size (µm2)
0.20
0.15
0.10
0.05
0.00
a
b
c
c
d
e
f
e
g
0d
7d
10d
15d
20d
7d
10d
15d
20d
D
N balanced
N balanced
N deprived
Recovery
Pgl/plastid
30
20
10
0
b,c
a,b
a,c
a
b,c
a,b
a
a,b
c
0d
7d
10d
15d
20d
7d
10d
15d
20d
E
N balanced
N balanced
N deprived
Recovery
LD size (µm2)
3
2
1
0
a
a
b
a
0d
7d
10d
15d
20d
7d
10d
15d
20d
F
N balanced
N balanced
N deprived
Recovery
LD/Cell Area (µm-2)
0.050
0.025
0.000
a
a,b
a,b
a,b
b
d
d
c
a,b
0d
7d
10d
15d
20d
7d
10d
15d
20d
G
MGDG
DGDG
PC
TAG
Phytyl-/Steryl-esters
Radioactivity (%)
Time (d)
N+
N-

Fig. 6: Effects of nitrogen starvation followed by a repletion period on Arabidopsis leaf cell ultrastructure and lipid metabolism. A. Scheme of the experimental procedure showing the labelling pulse of two-week-old plantlets, the 10 days of starvation on nitrogen depleted medium and the recovery phase for 10 supplemental days on nitrogen balanced medium. The control plantlets followed the same experimental procedure excepted that they were always transferred to nitrogen balanced medium. **B.** Ultrastructure of chemically fixed Arabidopsis leaves after 10 days of nitrogen starvation ($10N^-$) or 10 days of controlled growing conditions ($10N^+$) and 10 supplemental days of repletion ($20N^-$ or 20 N^+), observed by transmission electron microscopy. Scale bar: 1 µm; Quantification of the size of plastoglobules (**C**., cross-section area, in μm^2), number of plastoglobules per plastid (**D**.), size of LDs (**E**., cross-section area, in μm^2), and number of LDs per cell section area (**F**., μm^{-2}) in response to nitrogen starvation and after repletion. Bar = 1 µm. Pgl: plastoglobules. (more than 40 quantifications per parameter were obtained on at least 2 independent plants). **G.** Kinetics of the radiolabelling of MGDG, DGDG, phytyl-/steryl-esters and TAGs during nitrogen starvation and recovery phases. Grey area corresponds to nitrogen starvation period. Values are means ± SD of five biological replicates.

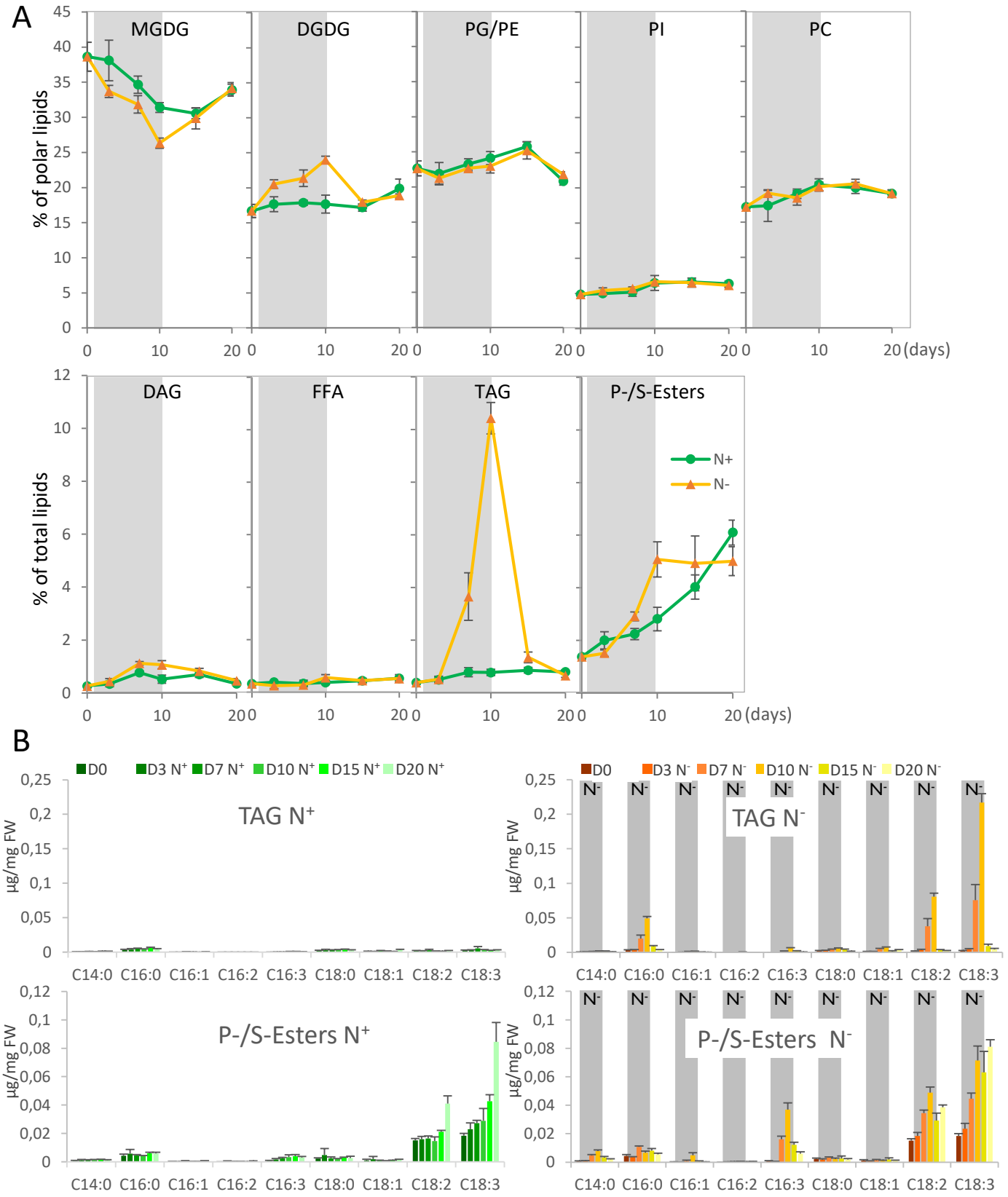

Figure 7: Glycerolipid analyses of Arabidopsis plantlets during nitrogen starvation and reversion. A. Glycerolipid distribution (in % of lipids); B. Neutral lipid fatty acid content (in µg/mg fresh weight). Two-week-old Arabidopsis plantlets were grown for 10 days on nitrogen balanced medium (N^+) or on nitrogen deprived medium (N^-, grey area), and their lipid composition determined by TLC/GC-FID at day 0 (D0), 3 (D3), 7 (D7) and 10 (D10). Plantlets were then transferred to nitrogen balanced medium for reversion, and their lipid composition similarly monitored after 5 days (D15) and 10 days (D20). Green bars: plantlets grown on nitrogen balanced medium; orange bars: plantlets submitted to nitrogen starvation for 10 days. For clarity reason, values of D0 are presented twice: with control (green) as well as with starved (orange) samples. Values are means ± SD of 4 biological replicates. P-/S-Esters : Phytyl-/Steryl-esters.

A. Phytyl-/Steryl-esters

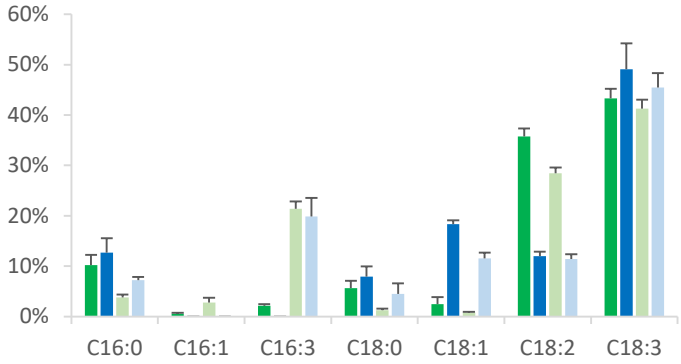

B. TAGs

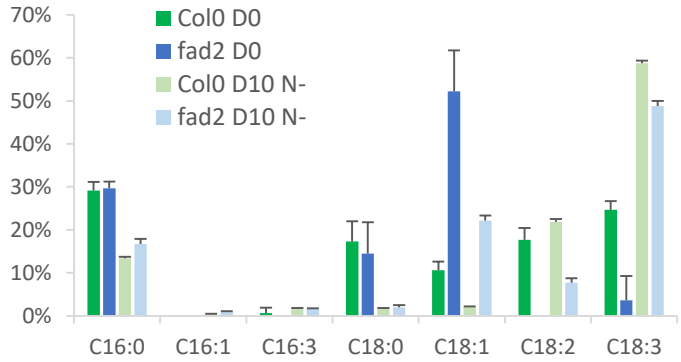

Figure 8: Fatty acid composition of neutral lipids from Col0 and *fad2* Arabidopsis plantlets during nitrogen starvation. Two-week-old Arabidopsis plantlets were grown for 10 days on nitrogen deprived medium and lipid extracted. The fatty acid compositions of phytyl-/steryl-esters (A) and TAGs (B) were determined by TLC/GC-FID before starvation (D0), and after 10 days of starvation (D10 N-). Green bars: *Col0* wild type; blue bars: *fad2* mutant. Values are means ± SD of 4 or 6 biological replicates for *Col0* or *fad2* respectively.

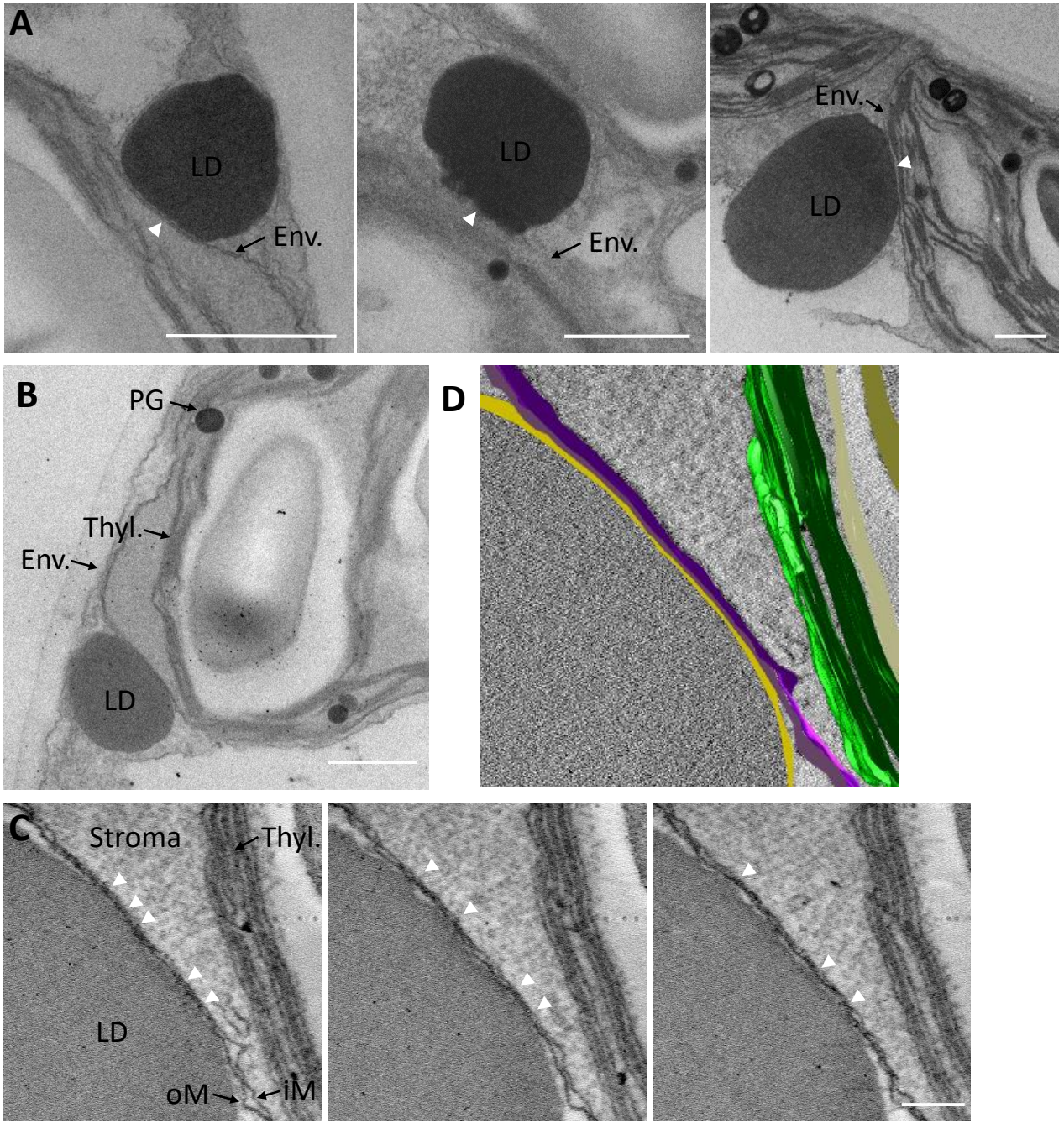

Figure 9: Morphology of the plastid-lipid droplet contact monitored by tomography. The ultrastructure was determined on chemically fixed Arabidopsis leaves subjected for 7 days to nitrogen starvation. A. Electron micrographs showing close proximity (white arrow heads) between LD and chloroplast. Bar: 0.5 µm. **B.** Overview of the contact between a chloroplast and a LD. Bar: 0.5 µm **C.** Tomographic slices of plastid-LD contact site shown in B., highlighting the appression of both plastid envelope membranes with the LD monolayer (white arrow heads). Bar: 0.1 µm. LD: lipid droplet; Env.: plastid envelope; iM: inner membrane of the plastid envelope; oM: outer membrane of the plastid envelope; PG: plastoglobule; Thyl.: thylakoids. The thickness of one tomographic slice is estimated to be around 0.23 nm. **D.** 3D segmentation of C; yellow: LD surface, light pink: outer envelope membrane, purple: inner envelope membrane, green: thylakoids, cream: starch granule.